How exerting control over outcomes affects the neural coding of tasks and outcomes

David Wisniewski[1], Birte Forstmann[2], Marcel Brass[1]

1 Department of Experimental Psychology, Ghent University, Belgium

2 Integrative Model-Based Cognitive Neuroscience Research Unit, University of Amsterdam, The Netherlands

Corresponding author

David Wisniewski

Department of Experimental Psychology, Ghent University

Henri Dunantlaan 2

9000 Gent

Tel: +32 (0)9 2649428

Email: david.wisniewski@ugent.be

Conflict of interest: The authors declare not competing financial interests.

Acknowledgements

We would like to thank Anita Tusche, Carlo Reverberi, and Ruth Krebs for valuable discussions on this project. This research was supported by the Research Foundation Flanders (FWO), the European Union's Horizon 2020 research and innovation program under the Marie Skłodowska-Curie grant agreement No 665501, FWO grant FWO.OPR.2013.0136.01, an ERC StG grant and NWO Vidi grant.

Abstract

Humans make choices every day, which are often intended to lead to desirable outcomes. While we often have some degree of control over the outcomes of our actions, in many cases this control remains limited. Here, we investigate the effect of control over outcomes on the neural correlates of outcome valuation and implementation of behavior, as desired outcomes can only be reached if choices are implemented as intended. In a value-based decision-making task, reward outcomes were either contingent on trial-by-trial choices between two different tasks, or were unrelated to these choices. Using fMRI, multivariate pattern analysis, and model-based neuroscience methods, we identified reward representations in a large network including the striatum, dorso-medial prefrontal cortex (dmPFC) and parietal cortex. These representations were amplified when rewards were contingent on subjects' choices. We further assessed the implementation of chosen tasks by identifying brain regions encoding tasks during a preparation or maintenance phase, and found them to be encoded in the dmPFC and parietal cortex. Importantly, outcome contingency did not affect neural coding of chosen tasks. This suggests that controlling choice outcomes selectively affects the neural coding of these outcomes, but has no effect on the means to reach them. Overall, our findings highlight the role of the dmPFC and parietal cortex in processing of value-related and task-related information, linking motivational and control-related processes in the brain. These findings inform current debates on the neural basis of motivational and cognitive control, as well as their interaction.

Significance statement

We all make hundreds of choices every day, and we want them to have positive consequences. Often, the link between a choice and its outcomes is fairly clear (healthy diet -> lower risk of cardiovascular disease), but we do not always have a high degree of control over the outcomes of our choices (genetic risk factors -> high risk despite a healthy diet). Control over outcomes is a key factor for decision-making, yet its neural correlates remain poorly understood. Here, subjects performed a value-based decision-making task, while we manipulated the degree of control over choice outcomes. We found that more control enhances the neural coding of choice outcomes, but had no effect on the implementation of the chosen behavior.

Introduction

Making decisions is an integral part of our life. Most of these choices are value-based, i.e. they are made with expected outcomes in mind. Value-based choices are made in separate stages: we first evaluate all options, and then select the option with the highest subjective value (Domenech et al., 2018). After implementing the chosen behavior (Rubinstein et al., 2001), predicted and experienced outcomes are compared, and prediction errors are computed (Matsumoto et al., 2007; Daw et al., 2011; Collins et al., 2017). This dopamine-mediated learning signal (Schultz, 2016) indicates the need to update our internal models of action-outcome contingencies (O'Reilly et al., 2013), which then leads to an adaption of future behavior.

This process is modulated by various properties of choice outcomes, e.g. their magnitude (Doya, 2008). However, one crucial aspect has received little attention in the past: to which degree we have direct control over the outcomes of our behavior. Clearly, whether or not we believe our choices to *cause* their outcomes affects decision-making considerably, yet previous work largely focused on direct control over behavior (Sperduti et al., 2011) and not its outcomes. Some previous research in non-human primates demonstrated that control over choice outcomes affects valuation processes in the brain. Choice-contingent rewards elicit different responses in the caudate (Izquierdo et al., 2004) and anterior cingulate cortex (Chudasama et al., 2013), as compared to non-contingent rewards (see also Elliott et al., 2004). Importantly, in order to lead to any rewarding outcome, the selected behavior needs to be implemented as intended first. Arguably, having control over choice outcomes should affect the means to reach those outcomes. One might expect chosen behaviors to be shielded more strongly against interference if outcomes are contingent on them (Dreisbach and Wenke, 2011), as not performing the behavior as intended is potentially costly. For non-contingent outcomes the need for shielding is lower, as e.g. executing the wrong behavior has no effect on outcomes (see Waskom et al., 2014 for a similar argument,

78 but Botvinick and Cohen, 2014). Previous work demonstrated that implementation of chosen actions,
79 which includes their maintenance and execution, is supported by a brain network including the
80 frontopolar (Soon et al., 2013), lateral prefrontal and parietal cortex (Zhang et al., 2013; Wisniewski et al.,
81 2016; Loose et al., 2017). Some initial evidence suggests that rewarding correct performance of externally
82 cued tasks indeed enhances their neural representations (Etzel et al., 2016), but this work did not address
83 the issue of varying degrees of control over choice outcomes.

84 Here, we report an experiment investigating the effects of control over choice outcomes on value-based
85 decision making. We used a value-based decision-making task to assess the effects of reward contingency
86 (choice-contingent vs. non-contingent rewards) on valuation and, more importantly, on choice
87 implementation. For this purpose, we used a combination of multivariate pattern analysis (MVPA, Haynes,
88 2015) and model-based neuroscience methods (Forstmann and Wagenmakers, 2015). We first
89 hypothesized that reward contingency affects the neural coding of outcome values in humans, as it does
90 in non-human primates (Izquierdo et al., 2004; Chudasama et al., 2013). We further assessed whether
91 implementation of chosen behavior (i.e. coding of chosen tasks) is similarly affected by contingency. We
92 hypothesized that the lateral prefrontal cortex, and especially the parietal cortex to play a key role in the
93 implementation of chosen behavior. The parietal cortex represents chosen tasks and actions (Wisniewski
94 et al., 2016; Domenech et al., 2018), subjective stimulus and action values (Sugrue, 2004; Kahnt et al.,
95 2014), as well as associations between choice options and their outcomes (Wisniewski et al., 2015a). Using
96 MVPA, we tested whether task representations in these brain regions were enhanced when rewards were
97 choice-contingent vs when they were not.

Materials and Methods

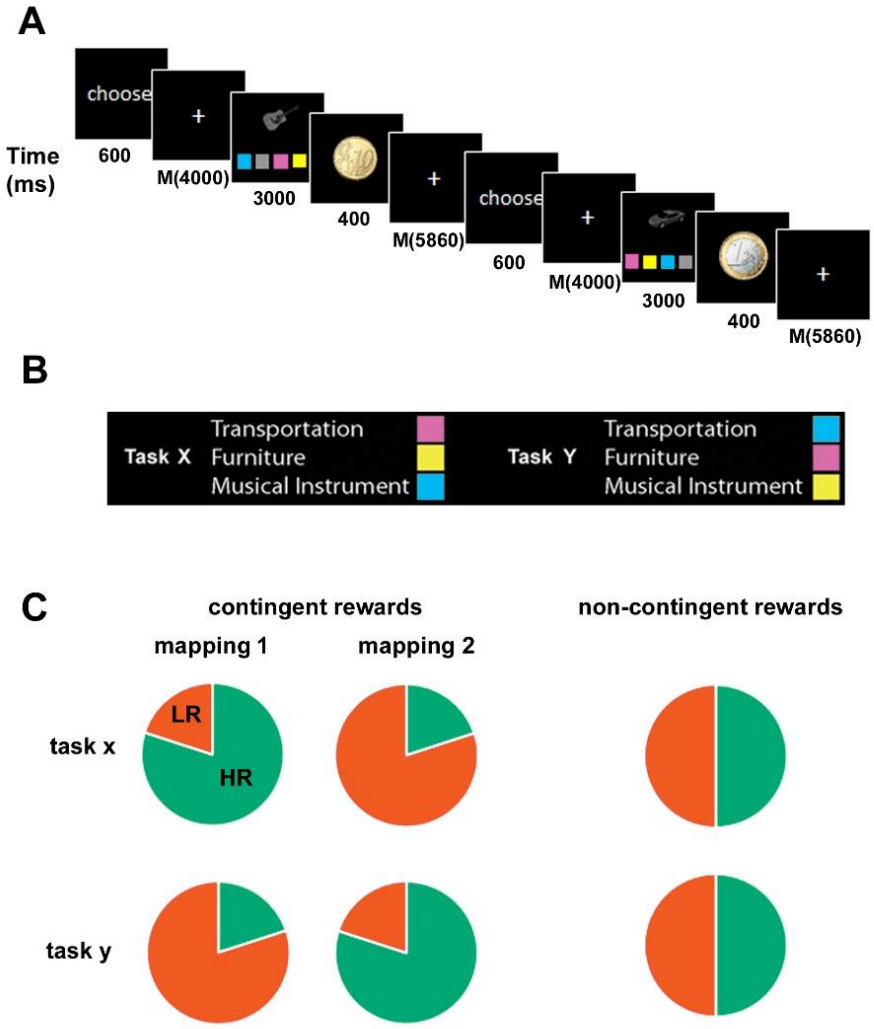

Figure 1. Experimental paradigm. **A.** Trial structure. Each trial started with the cue 'choose' presented on screen. After a variable delay, the task screen was presented for a fixed duration. Reward feedback was presented subsequently after each trial. All trials were separated by variable inter trial intervals. **B.** Tasks. Subjects were instructed to identify the visual object presented on screen, and press a corresponding colored button. The object-category to color mappings are depicted here. Note that the specific mappings were counterbalanced across subjects. Which task was implemented in each trial was chosen freely by the subjects. **C.** Reward contingencies. In contingent (RC) trials, one task always yielded a high reward with a higher probability (80%) than the other task (20%). Which specific task was currently the high-reward task depended on the current task-reward-mapping, which changed according to a probabilistic reversal learning procedure (see Materials and Methods for more details). In non-contingent (NCR) trials, the chance to receive a high and low reward were equal, irrespective of the chosen task.

Participants

A total of 42 subjects participated in this experiment (20 males, 21 females, 1 other). The average age was 22.6 years (min = 18, max = 33 years), 41 subjects were right-handed, one was left-handed. All subjects had normal or corrected-to-normal vision and volunteered to participate. Subjects gave written informed consent and received between 45€ and 55€ for their participation. The experiment was approved by the local ethics committee. Seven subjects showed excessive head movement in the MR scanner (>4mm) and were excluded. All reported analyses were thus performed on a sample of 35 subjects. Despite the fact that the multivariate analyses performed in this experiment (see below for details) show notoriously small effects (Bhandari et al., 2018), we believe to have sufficient statistical power with the given sample size.

Experimental Design

The experiment was programmed using PsychoPy (version 1.85.2, psychopy.org, RRID:SCR_006571, Peirce, 2007)). In each trial, subjects were free to choose between two different tasks, and could either earn a high or a low reward for correct performance. The paradigm is described in more detail below.

Trial structure

Each trial started with the presentation of a fixation cross centrally on-screen for 300ms (Figure 1 A). This was followed by the presentation of a choice cue, the word 'CHOOSE', for 600ms. This cue instructed subjects to freely choose one of the two tasks to perform in this trial. After a variable delay period (2000-6000ms, mean delay duration = 4000ms), the task screen was presented for a total of 3000ms. In this experiment, we used the same tasks as (Wisniewski et al., 2015b), in order to better compare current results to this previous experiment on value-based decision-making. The task screen consisted of a visual object presented centrally on screen (Figure 1 B). This object was picked pseudo-randomly out of a pool of 9 different objects in 3 categories: musical instruments, furniture, means of transportation. Below, 4 colored squares were presented (magenta, yellow, cyan, gray), with the square positions being mapped

134 onto 4 buttons, operated using the left and right index and middle fingers. Subjects were given the option
135 to choose which of two stimulus-response-mappings to apply to the presented object. For instance, in
136 task 'X', means of transportation were associated with the magenta, furniture with the yellow, and
137 musical instruments with the cyan button. In task 'Y', means of transportation were associated with the
138 cyan, furniture with the magenta, and musical instruments with the yellow button. Thus, depending on
139 the chosen task and the presented object, one of the colored buttons was correct for each task, and
140 subjects were instructed to react as quickly and accurately as possible. We inferred subjects' choices from
141 their responses. Note, that the grey button was never task-relevant and was merely included to balance
142 left and right hand responses. Furthermore, the mapping of the colored buttons on screen was pseudo-
143 randomized in each trial, preventing subjects from preparing a specific motor response before the onset
144 of the task screen. The specific stimulus-response-mappings called *task X* and *task Y* were counter-
145 balanced across subjects. Subsequently to the task-screen presentation, subjects were given trial-by-trial
146 reward feedback, by presenting either an image of a 1€ coin (high reward), a 10€cent coin (low reward),
147 or a red circle (no reward). The feedback was presented for 400ms. After a variable inter-trial-interval
148 (4000-14000ms, geometrically distributed, mean duration = 5860ms), the next trial began.

149 Reward conditions

150 Subjects were rewarded for correct performance on every trial. There were a total of two different reward
151 conditions: contingent rewards (CR) and non-contingent rewards (NCR). In the NCR condition, the chosen
152 reward in each trial was determined randomly. Irrespective of the chosen task, subjects had a 50% chance
153 of receiving a high and a 50% chance of receiving a low reward (Figure 1 C). Subjects were instructed to
154 choose tasks randomly in this condition, by imagining flipping a coin in their head in each trial (Zhang et
155 al., 2013). In the CR condition, subjects performed a probabilistic reward reversal-learning task, similar to
156 (Hampton and O'Doherty, 2007). In each trial, one task led to a high reward with an 80% and a low reward
157 with a 20% probability (high-reward task, HR). These probabilities were reversed for the other task (low-

158 reward task, LR), e.g., in a specific trial, *task X* might be the HR task, while *task Y* might be the LR task.
159 Subjects were unaware which of the two tasks was the HR task, and needed to learn this from the reward-
160 feedback provided after each trial. Once they chose the HR task on 3 consecutive trials, the mapping of
161 rewards onto tasks reversed with a chance of 25% on each subsequent trial, e.g., whereas before *task X*
162 was the HR and *task Y* the LR task, now *task X* was the LR and *task Y* the HR task. Again, subjects were
163 unaware of this change in reward-contingencies, and needed to learn when such a switch occurred from
164 the reward-feedback provided at the end of each trial.

165 At the end of the experiment, 15 trials were chosen randomly, and whichever reward was earned in these
166 trials was paid out as a bonus payment to the subjects. One half of these trials was chosen from CR trials,
167 the other from NCR trials, which was communicated to the subjects in order to ensure that both
168 conditions are equally salient. Thus, subjects were motivated to maximize the reward in CR trials, choosing
169 the HR task as often as possible. Given that rewards were randomly chosen in NCR trials, they had no
170 influence over the earned reward in this condition.

171 This reward manipulation was chosen to manipulate the degree of control subjects had over the outcome
172 of their choices. In CR trials subjects made choices that were directed at earning as much money as they
173 could, by learning the changing reward contingencies and thus controlling reward outcomes. In NCR trials,
174 subjects were unable to control outcomes through their choices, as there were no contingencies to learn.
175 This allowed us to assess effects of control over outcomes on valuation and implementation processes. A
176 second important reason for manipulating reward 'relevance' instead of reward presence (as in Etzel et
177 al., 2016), was that this allowed us to assess specific reward effects on valuation and implementation
178 processes. When contrasting choices in which subjects could earn a reward, with choices in which no
179 reward is present (e.g. Libet et al., 1983; Soon et al., 2008), any difference between these conditions might
180 arise from unspecific processes merely correlated with the presence of reward, like attentional or motor
181 preparation (Kahnt et al., 2014). This is mainly because strong differences in expected outcomes

immediately trigger these preparatory processes selectively in rewarded trials. In contrast, when rewards are always present, but only sometimes contingent on choices, reward expectations are much more similar across conditions. In fact, if a subject chose tasks randomly in all trials, the expected value would be identical in both reward conditions. Thus, only specific reward-related effects, like the fact that reward outcomes are a relevant factor for making choice only in CR trials, can explain potential differences between CR and NCR trials.

Design

Subjects performed 5 identical runs of this experiment, with 60 trials each. Each run contained 2 blocks with CR and 2 blocks with NCR trials. The length of each block was between 10 and 14 trials, and all trials were all separated by a long and variable ITI. CR and NCR blocks alternated and block order was counterbalanced across runs for each subject. Each block started with either 'Contingent block now starting' or 'Non-contingent block now starting' presented on screen for 5000ms. This mixed blocked and event-related design minimized cross-talk and interference between the reward conditions, and allowed us to estimate cleaner neural signals.

Each run also contained 20% (n=12) catch trials. In these trials, subjects were externally cued which task to perform, by presenting the words 'TASK X' or 'TASK Y' instead of the 'CHOOSE' cue. The delay between cue and task execution was 1000ms in these trials. Catch trials were included to prevent subjects from choosing all tasks in a block at its beginning. For instance, in an NCR block, subjects could theoretically decide upon a whole sequence of tasks at the beginning of that block (e.g. X,X,X,Y,X,Y,Y,X,...), and then only implementing that fixed sequence in each trial. In order to encourage subjects to make a conscious choice in each individual trial, catch trials were included. These trials would frequently disrupt any planned sequence of task choices, making such a strategy less feasible. In order to increase the salience of these catch trials, subjects always received a high reward for correct performance. Catch trials were excluded from all analyses.

206 Furthermore, we ensured that the reward condition was not correlated with any other design variable
207 (target stimulus, delay duration, button mapping, ITI duration), in order to ensure that estimated neural
208 signals were not confounded. Lastly, multivariate pattern analyses can be biased if signal estimates are
209 not based on trials which are IID. Thus we ensured that conditions of the previous trial were not predictive
210 of the current trial, to make each trial as independent of all other trials as possible.

211 ## Training session

212 Subjects were familiarized with the task in a separate training session outside the MR scanner, lasting
213 about 1h10min. Subjects first learned to perform the two tasks, were then instructed about the reward
214 conditions and lastly performed 3 runs of the full experiment (as described above). This training session
215 was performed to minimize learning effects during the MR session, which can be detrimental to
216 multivariate pattern analyses. Training sessions were scheduled between 1-5 days before the MR session.
217 Just before the start of the MR session, subjects performed 10 trials of the task in the MR scanner, in order
218 to familiarize themselves with the novel environment. These trials were not analyzed.

219 ## Additional measures

220 After completing the MR session, subjects filled in multiple questionnaires. They answered custom
221 questions (e.g., How believable were the instructions? How different were the reward conditions? How
222 difficult was making a choice between the two tasks? How difficult was performing the two tasks? Was
223 one task more difficult than the other? At which point in time did you choose the task to perform in each
224 trial?), and the following questionnaires: behavioral inhibition / activation scale (BISBAS, Carver and
225 White, 1994), need for cognition (NFC, Cacioppo et al., 1984), sensitivity to reward / punishment (SPSRQS,
226 Torrubia et al., 2001), and impulsivity (BIS11, Patton et al., 1995). We also acquired pupil dilation data
227 while subjects performed the experiment in the MR scanner. Pupil dilation data is not the focus of the
228 current paper, and is not reported.

Image acquisition

fMRI data was collected using a 3T Magnetom Trio MRI scanner system (Siemens Medical Systems, Erlangen, Germany), with a standard thirty-two-channel radio-frequency head coil. A 3D high-resolution anatomical image of the whole brain was acquired for co-registration and normalization of the functional images, using a T1-weighted MPRAGE sequence (TR = 2250 ms, TE = 4.18 ms, TI = 900 ms, acquisition matrix = 256 × 256, FOV = 256 mm, flip angle = 9°, voxel size = 1 × 1 × 1 mm). Furthermore, a field map was acquired for each participant, in order to correct for magnetic field inhomogeneities (TR = 400 ms, TE_1 = 5.19 ms, TE_2 = 7.65 ms, image matrix = 64 x 64, FOV = 192 mm, flip angle = 60°, slice thickness = 3 mm, voxel size = 3 x 3 x 3 mm, distance factor = 20%, 33 slices). Whole brain functional images were collected using a T2*-weighted EPI sequence (TR = 2000 ms, TE = 30 ms, image matrix = 64 × 64, FOV = 192 mm, flip angle = 78°, slice thickness = 3 mm, voxel size = 3 x 3 x 3 x mm, distance factor = 20%, 33 slices). Slices were orientated along the AC-PC line for each subject.

Statistical Analysis

Data Analysis: Behavior

All behavioral analyses were performed in R (RStudio version 1.1.383, RRID:SCR_000432, www.rstudio.com). We first characterized subjects' performance by computing error rates and reaction times (RT). We tested for potential effects of reward condition on error rates using a Bayesian two-sided paired t-tests (using *ttestBF* from the BayesFactor package in R). Error trials, and trials with RTs <300ms were removed from the data analysis. In order to identify potential effects of task and reward condition on RTs, we performed a Bayesian repeated measures ANOVA (using *anovaBF* from the BayesFactor package in R). This ANOVA included the factors task (X, Y) and reward (CR, NCR), and outputs Bayes Factors (BF) for all main effects and interaction terms. We did not expect tasks to strongly affect RTs, but did expect RTs to be lower in the CR condition, as compared to the NCR condition.

The Bayesian hypothesis testing employed here allows quantifying the evidence in favor of the alternative hypothesis (BF10) *and* the null hypothesis (BF01), allowing us to conclude whether we find evidence for or against a hypothesized effect, or whether the current evidence remains inconclusive (Rouder, Speckman, Sun, Morey, and Iverson, 2009). Unfortunately, in classical frequentist hypothesis testing we are unable to provide evidence for the null hypothesis in a similar way (Wagenmakers, 2007). In line with previous research (e.g. Andraszewicz et al., 2015; Mertens and De Houwer, 2016), we considered BFs between 1 and 0.3 as anecdotal evidence, BFs between 0.3 and 0.1 as moderate evidence, and BFs smaller than 0.1 as strong evidence against a hypothesis. BFs between 1 and 3 were considered as anecdotal evidence, BFs between 3 and 10 as moderate evidence, and BFs larger than 10 as strong evidence for a hypothesis. Although our conclusions are based solely on the BFs, we also provide frequentists statistical test outcomes for the interested reader.

Given that subjects were free to choose between the two tasks, some subjects might have shown biases to choosing one of the two tasks more often (although that would not have led to a higher overall reward, if anything biases should lower overall rewards). In order to quantify biases, we computed the proportion of trials in which subjects chose task X, separately for the CR and NCR conditions, and tested whether this value differed from 50% using a two-sided Bayesian t-test. The output BF was interpreted in the same way as in the previous analysis.

Choices in CR trials were assessed two-fold. First, we quantified how well subjects performed the probabilistic reversal learning task. If subjects were reliably able to determine which of the two tasks was currently the HR task, they should have chosen that task more often than expected by chance (50%). Thus the proportion of HR task choices in CR trials is our main measure of how successful subjects were in performing the task. This measure was compared to chance level using a one-sided Bayesian t-test. Furthermore, we expected the proportion of HR choices to be higher in CR, than in NCR trials (where it should be 50%). This was tested using a paired one-sided Bayesian t-test.

Second, we assessed whether subjects were able to learn and update reward contingencies in the reversal learning task. Reinforcement learning (RL) theory suggest that such learning can take place by comparing received rewards with expected rewards, which are computed from the reward history (Sutton and Barto, 1990; Collins et al., 2017). Discrepancies between actual and expected rewards (reward prediction errors, RPE) are thought to signal surprise in the brain and to guide adjustment of behavior (Daw and Doya, 2006), a process which relies on dopaminergic signals in the midbrain (Pessiglione et al., 2006; Schultz, 2016). Here, we fitted a RL model to the choice data of each subject (separately for CR and NCR trials) in order to assess the learning process. Fitted RL models used simple delta-rule learning (as implemented in the *rlfit* package in Matlab, https://github.com/jmxpearson/rlfit). For each task choice *c* the expected reward *Q(c)* was learned from the reward history by comparing the expected and observed rewards at trial *t*:

$$Q_{t+1}(c) = Q_t(s) + \alpha \, X \, \delta_t$$

with $\delta_t = r_t - Q_t(c)$ being the RPE, and α being the learning rate. Choices were generated following a softmax choice function (as implemented in the rlfit package). The parameters were fitted over n = 10 iterations, with random starting values in each iteration. Learning rates were fitted with constraints [0, 1]. In order to assess the model fit, we also estimated a 'null' model for each subject. In this model, we again estimated expected outcomes and RPEs using the same algorithm described above, only fixing the learning rate to 0. The null model thus assumed that subjects do not learn changing reward contingencies, and we expected our RL model to outperform this null model. Model fit was assessed using the AIC and BIC (Burnham and Anderson, 2004). We also assessed an alternative 'hybrid' model, in which learning rates are allowed to vary on a trial-by-trial basis, instead of being fixed for each subject (Bai et al., 2014). It has been argued that such a model better captures behavior in probabilistic reversal learning tasks. In our experiment the simple delta-rule learning model outperformed the more complex hybrid model (as assessed using AIC and BIC), and results from the hybrid model were not assessed further.

For each subject, the learning rate was extracted from the best-fitting model. We expected learning rates to be higher in CR than in NCR trials. In CR trials, the specific reward contingencies changed frequently, and thus subjects needed to update their contingency representations frequently as well. The learning rate in CR trials was also expected to correlate with successful task performance (% high reward choices), given that the reversal learning task can only be performed well if the represented reward contingencies change over time. In NCR trials, we expected learning rates to be low and uncorrelated with choice performance, because reward outcomes were randomly chosen and there were no contingencies to learn.

Choices in NCR trials were assessed by testing whether subjects were able to choose tasks randomly in these trials. For this purpose, we computed the distribution of run lengths for each subject, i.e., the number of trials subjects chose to consecutively perform the same task. If subjects chose tasks randomly, this distribution can be expected to follow an exponential distribution (cf. Arrington and Logan, 2004; Soon et al., 2008). The average run length was computed for each subject, separately for CR and NCR trials, and compared to the expected run length under random choice behavior. We expected subjects to show longer runs in CR than in NCR trials, given that the probabilistic reward reversal learning task encourages subjects to perform the same task repeatedly. This was again tested using a one-sided Bayesian t-test.

Data Analysis: fMRI

fMRI data analysis was performed using Matlab (version R2014b 8.4.0, RRID:SCR_001622, The MathWorks) and SPM12 (RRID:SCR_007037, www.fil.ion.ucl.ac.uk/spm/software/spm12/). Raw data was imported according to BIDS standards (RRID:SCR_016124, http://bids.neuroimaging.io/). In order to assess which brain regions contained information about reward outcomes and task choices, raw data was unwarped, realigned and slice time corrected. It was then entered into a first level general linear model analysis (GLM, Friston et al., 1994), and subsequently into a multivariate pattern analysis (MVPA, Cox and

Savoy, 2003; Kriegeskorte et al., 2006; Haxby, 2012; Haynes, 2015). In order to assess which brain regions represented reward-learning signals, raw data was unwarped, realigned, slice time corrected, normalized, and smoothed. It was then entered into a GLM, adding reward prediction errors as a regressor. Results were analyzed using a mass-univariate approach. Full details of the analyses can be found below.

Neural processing of reward

Multivariate decoding of reward outcomes

In a first step, we assessed whether we can replicate previous findings demonstrating contingency effects on reward processing (Tricomi et al., 2004). For this purpose, we estimated a GLM for each subject. For each of the 5 runs we added regressors for each combination of reward value (high vs low) and contingency (CR vs NCR). All regressors were locked to the feedback onset, the duration was set to 0. Regressors were convolved with a canonical haemodynamic response function (as implemented in SPM12). Estimated movement parameters were added as regressors of non-interest to this and all other GLMs reported here.

Baseline decoding: In a next step, we performed a decoding analysis on the parameter estimates of the GLM. A support-vector classifier (SVC, see Cox and Savoy, 2003; Mitchell et al., 2004; Kamitani and Tong, 2005), as implemented in *The Decoding Toolbox* (Hebart et al., 2014), was used using a fixed regularization parameter (C = 1). We performed searchlight decoding (Kriegeskorte et al., 2006; Haynes et al., 2007), which looks for information in local spatial patterns in the brain and makes no a prior assumptions about informative brain regions. A sphere with a radius of 3 voxels was defined around each measured voxel, and parameter estimates for high rewards (both in CR and NCR trials), and for low rewards (again, both in CR and NCR trials) were extracted within that sphere, separately in each run. 4 out of 5 runs were used to train the SVC to distinguish the neural patterns of high and low rewards. Classifier performance was then tested on the remaining, independent run. This procedure was repeated until each run was left out once,

345 resulting in a 5-fold cross-validation and countering potential problems with overfitting. Mean prediction
346 accuracy was calculated across all folds and written into the center voxel of the sphere. This was repeated
347 for each measured voxel in the brain, resulting in a 3D accuracy map. These maps were computed for each
348 subject, normalized to a standard space (Montreal Neurological Institute template as implemented in
349 SPM12), and smoothed (Gaussian kernel, FWHM = 6mm) in order to account for potential differences in
350 information localization across subjects. Group analyses were performed using a random effects model
351 on the accuracy maps, using voxel-by-voxel t-tests against chance level (50%). The chance level was
352 subtracted from all reported accuracy values. A statistical threshold of $p<0.0001$ (uncorrected) at the voxel
353 level, and $p<0.05$ (family-wise error corrected) at the cluster level was applied to all analyses. This
354 threshold is sufficient to rule out inflated false-positive rates in fMRI analyses (Eklund et al., 2016). Any
355 regions surpassing this threshold were used as masks for the following decoding analyses (an approach
356 previously used by (Loose et al., 2017). Given that we are mainly interested in *differences* between the
357 baseline and other analyses, this comparison does not constitute a case of double dipping. Please also
358 note that this analysis is sensitive to differences in outcome value, but might possibly also identify brain
359 regions related to unspecific preparatory (e.g., attentional) processes. Although preparatory processes
360 should be identical in CR and NCR trials, due to the fact that the same high and low rewards were given in
361 both conditions, we cannot fully exclude such effects either if subjects were generally more motivated to
362 perform CR than NCR trials. The underlying cause of any observed effects remain differences in reward
363 outcomes however.

364 *Differences in reward outcome coding*: Although the baseline decoding analysis should have the maximum
365 power to detect any outcome-related brain regions, results do not allow us to conclude whether outcome
366 processing differed between CR and NCR trials. For this purpose, we repeated the decoding analysis, now
367 only using CR trials, and only NCR trials, respectively. If contingent rewards indeed enhance encoding of
368 reward outcomes in the brain, we should see higher accuracies in the CR than in the NCR decoding

analysis. Please note, that we only used half the number of trials as before, thus considerably reducing the signal-to-noise ratio in these analyses. We thus expected lower statistical power and smaller effects.

Similarities in in reward outcome coding: Previous work demonstrated that not all brain regions show a contingency-related modulation of value signals (Elliott et al., 2004), and we thus tested whether some brain regions encoded reward outcomes invariantly across the contingency conditions. We trained a classifier to discriminate between high and low reward outcomes in the CR condition, and tested its performance in the NCR condition, and vice versa. This resulted in two accuracy maps per subject, which were averaged and then entered into a group analysis just like in the previous analyses. Importantly, only brain regions where patterns do not differ across both contingency conditions will show above-chance accuracies in this analysis. This so-called cross classification analysis can be used to identify brain regions in which outcome representations are invariant with respect to the contingency manipulation employed here (see also Kaplan et al., 2015), thus providing positive evidence for contingency-invariant coding of reward outcomes.

Neural correlates of reward-learning signals

While the previous analyses investigated the neural correlates of processing the hedonic value of reward outcomes, here, we directly assessed whether reward-learning signals are affected by reward contingency. Reward prediction errors (RPE) act as learning signals in our reversal learning task (Matsumoto et al., 2007; Daw et al., 2011). They indicate the need to update the internal model of the current task-reward associations (e.g. task X = high reward task). In order to identify brain regions encoding this important reward signal, we used a model-based fMRI approach (O'Doherty et al., 2007; Forstmann and Wagenmakers, 2015). In model-based fMRI, a computational model fitted to behavioral data is used to construct regressors, which are then used to estimate GLMs on fMRI data. This approach links brain and behavior in a mechanistic framework and has been used successfully in a number of

392 different settings (for an overview see Forstmann and Wagenmakers, 2015). We used the reinforcement
393 learning models fitted to the behavioral data, and computed trial-by-trial RPEs from the best fitting model
394 of each subject. We then estimated two separate GLMs, one for CR trials and one for NCR trials, on
395 normalized and smoothed raw data. For each of the 5 runs, we added one regressor (duration = 0) locked
396 to the onset of the feedback screen of each trial. Prediction errors should be strongest at this point in
397 time. We added the trial-by-trial RPEs as a parametric modulator, allowing us to identify brain regions
398 correlating with RPE signals. As before, regressors were convolved with a canonical haemodynamic
399 response function. For each subject, a t-contrast map was computed to identify regions reflecting RPEs.
400 These maps were then entered into a group level random effects analysis (within-subjects ANOVA with
401 the factor contingency (CR, NCR)) in order to identify brain regions where prediction errors were
402 modulated by reward contingency. Results were thresholded at $p < 0.001$ (uncorrected) at the voxel level,
403 $p < 0.05$ (FWE corrected) at the cluster level.

404 *Multivariate decoding of tasks*

405 All analyses described above aimed at assessing effects of reward contingency on reward processing. Now,
406 we turn to also test whether any such potential effects could be demonstrated on the implementation of
407 chosen behavior in the brain. For this purpose, we assessed which brain regions encoded the chosen tasks.
408 Two GLMs were estimated for each subject, one modelling task-related brain activity at the time of
409 decision-making, and one modelling activity during a subsequent maintenance phase. It has been shown
410 that formation and maintenance of intentions rely on partly dissociable brain networks (Bunge et al.,
411 2003; Gilbert, 2011), and our design allowed us to estimate independent signals related to both epochs
412 as they were separated by a variable inter-trial-interval.

413 In the first GLM ($GLM_{maintenance}$), for each of the 5 runs we added regressors for each combination of chosen
414 task (task X, task Y) and reward contingency (CR, NCR). All 4 regressors were locked to the cue onset, the

duration was set to cover the whole delay period. Please note that due to the jittered delay period duration, the modelled signals were dissociated from the task execution and feedback presentation. These boxcar regressors were then convolved with a canonical haemodynamic response function. This model is highly similar to the model used in (Wisniewski et al., 2016), where subjects were also free to choose one of two different tasks in each trial, making current results highly comparable to this previous study. In sum, this model estimated task-specific brain activity during intention maintenance, i.e. while subjects had to represent their intention to perform a specific chosen task, without yet being able to prepare a specific motor response. A second GLM was estimated ($GLM_{decisiontime}$), in order to extract task-specific brain activity at the time subjects made their choice which of the two tasks to perform. Note that although the cue suggested that subjects should make a task choice at that point in time, there is no strong way of controlling the exact point in time at which choices were made. In fact, choices could have been made earlier than the presentation of the choice cue. It has been shown before that under free choice conditions, subjects choose a task as soon as all necessary information to make a choice is available (Hampton and O'Doherty, 2007; Wisniewski et al., 2015b). In this experiment, this time point is the feedback presentation of the previous trial. At this point, subjects can judge whether they e.g. chose the HR or LR task and determine which of the two tasks to perform in the next trial. We used this approach successfully in a previous experiment (Wisniewski et al., 2015b), again making current results highly comparable with these previous findings. All further task decoding analyses were performed on both GLMs.

Baseline decoding: The task decoding analyses followed the same logic as the reward outcome analyses described above. We first performed a searchlight decoding analysis (radius = 3 voxels, C = 1), contrasting parameter estimates for tasks X and Y in all trials (CR and NCR combined). This analysis has the maximum power to detect any brain regions containing task information, which can be notoriously difficult (Bhandari et al., 2018). Resulting accuracy maps were normalized, smoothed (6mm FWHM), and entered

439 into a random effects group analysis (t-test vs chance level, 50%). Results were thresholded at $p<0.001$
440 (uncorrected) at the voxel level, and $p<0.05$ (family-wise error corrected) at the cluster level. Again,
441 regions surpassing this threshold were used to define functional regions-of-interest for the following
442 decoding analyses (see Loose et al., 2017).

443 *Differences in task coding*: In order to assess whether task coding is modulated by reward contingency,
444 we repeated the decoding analysis separately for CR and NCR trials. If contingent rewards indeed increase
445 task shielding in the brain, we should see higher accuracies in the CR than in the NCR decoding analysis.
446 This effect should be especially pronounced if both tasks are similar and easily confused, which is the case
447 in our experiment. Please note, that we again only used half the number of trials as before, reducing the
448 signal-to-noise ratio in these analyses. We thus expected lower statistical power and smaller effects.

449 *Similarities in task coding*: Some previous work suggests that tasks are encoded in a context-invariant
450 format in the brain (Zhang et al., 2013; Wisniewski et al., 2016), and we directly tested whether this was
451 also true in this experiment. Using a cross-classification (xclass) approach, we trained a classifier on CR
452 trials and then tested it on NCR trials (and vice versa). And brain regions showing above chance decoding
453 accuracies in this analysis provides positive evidence of task coding that is invariant with respect to
454 contingent vs non-contingent reward outcomes.

455 *Region of interest analyses*: We also assessed task information in a number of a priori defined regions of
456 interest (ROI). First, we attempted to replicate results from one of our previous experiments (Wisniewski
457 et al. 2015). There, the dmPFC has been found to encode task choices at the time of decision-making. We
458 extracted this functional ROI, and tested whether we could replicate the finding in this independent and
459 larger sample. Although the overall design differed considerably (e.g. 3 vs 2 tasks, changing reward
460 outcomes vs changing task difficulty), both studies used the same object-categorization task. Second, two
461 previous experiments found task information to be maintained in the fronto-parietal cortex in a context

462 invariant fashion (Loose et al. 2017; Wisniewski et al. 2016). In one paper, task coding was invariant with
463 respect to freely chosen vs. externally cued tasks (Wisniewski et al. 2016), while in the other paper, task
464 coding was invariant with respect to high vs. low control demands (Loose et al. 2017). If we were to show
465 that the regions identified in these two experiments also encode tasks invariantly across reward
466 contingency conditions, that would provide additional evidence for general, context invariant task coding
467 in the fronto-parietal cortex. We thus extracted functional ROIs from both papers (Wisniewski et al. 2016:
468 left parietal cortex, left PFC, Brodman area 8; Loose et al. 2017: left parietal cortex, left PFC), and tested
469 this hypothesis in this independent data-set. For all ROIs defined, we extracted accuracy values for all
470 voxels within the ROI, which were then averaged. One-sided Bayesian t-tests across subjects were
471 performed to assess whether they were above chance.

472 *Control analyses*: In order to further corroborate the reliability of our results, we performed a number of
473 control analyses. It has been pointed out before, that RT effects might partly explain task decoding results
474 (Todd et al., 2013), although others were unable to show any such effects (Woolgar et al., 2014;
475 Wisniewski et al., 2015b). Given that we expected RTs to differ across reward conditions, we decided to
476 conservatively control for RTs effects. First, we repeated the GLM estimation, only adding reaction times
477 as an additional regressor of non-interest. We then repeated the main decoding analyses, and tested
478 whether accuracy values differed significantly. If RTs indeed explain our task decoding results, we should
479 see a reduction in decoding accuracies when RT effects were regressed out of the data.

480 Furthermore, it is possible that some subjects exhibit excessive error rates or have a strong bias to choose
481 one task more often than the other. High error rates might decrease the signal-to-noise ratio and thus
482 affect observed results. Very strong choice biases might have a similar effect, in extreme cases subjects
483 might have performed only one of the two tasks in a given run (although this was unlikely). In order to
484 ensure that we had enough trials to estimate each regressor, we first excluded subjects with excessively
485 high error-rates (more than 1.5*IQR above average), and then excluded subjects with strong choice biases

(more than 1.5*IQR above average). We then tested whether each regressor in all remaining subjects could be estimated from at least 6 trials. If a regressor could only be estimated from fewer trials, that run was excluded from the analysis. Subjects in which more than 1 run was thusly excluded were altogether excluded from the analysis. These criteria were highly similar to the criterion used in (Wisniewski et al., 2015b), which proved an effective control. After excluding these subjects, we repeated the main analyses on the remaining subjects and tested whether they differed from the analysis including all subjects.

Two further control analyses were performed to confirm the validity of the decoding procedure used. First, we performed a ROI decoding analysis on a brain region that is not related to task-performance in any way, expecting accuracies to be at chance level. We chose the primary auditory cortex for this purpose, defined using the WFU_pickatlas tool (https://www.nitrc.org/frs/?group_id=46, RRID: SCR_007378). Second, we tested whether our chance level was indeed 50%, or whether it was biased. For this purpose, we performed a permutation analysis (as implemented in the Decoding Toolbox). We repeated the baseline decoding analysis 1000 times for each subject, only randomly assigning the test labels in each of the 1000 permutations. A null distribution was calculated from these permutations separately for each subject, and the mean accuracy value of the null distribution served as an empirical estimate of the chance level. In order to test whether the estimated chance level deviated from 50%, we performed a two-sided Bayesian t-test. Additional exploratory analyses were performed to assess possible correlations between behavioral measures, questionnaires, and fMRI results (Figure 2–1).

Results

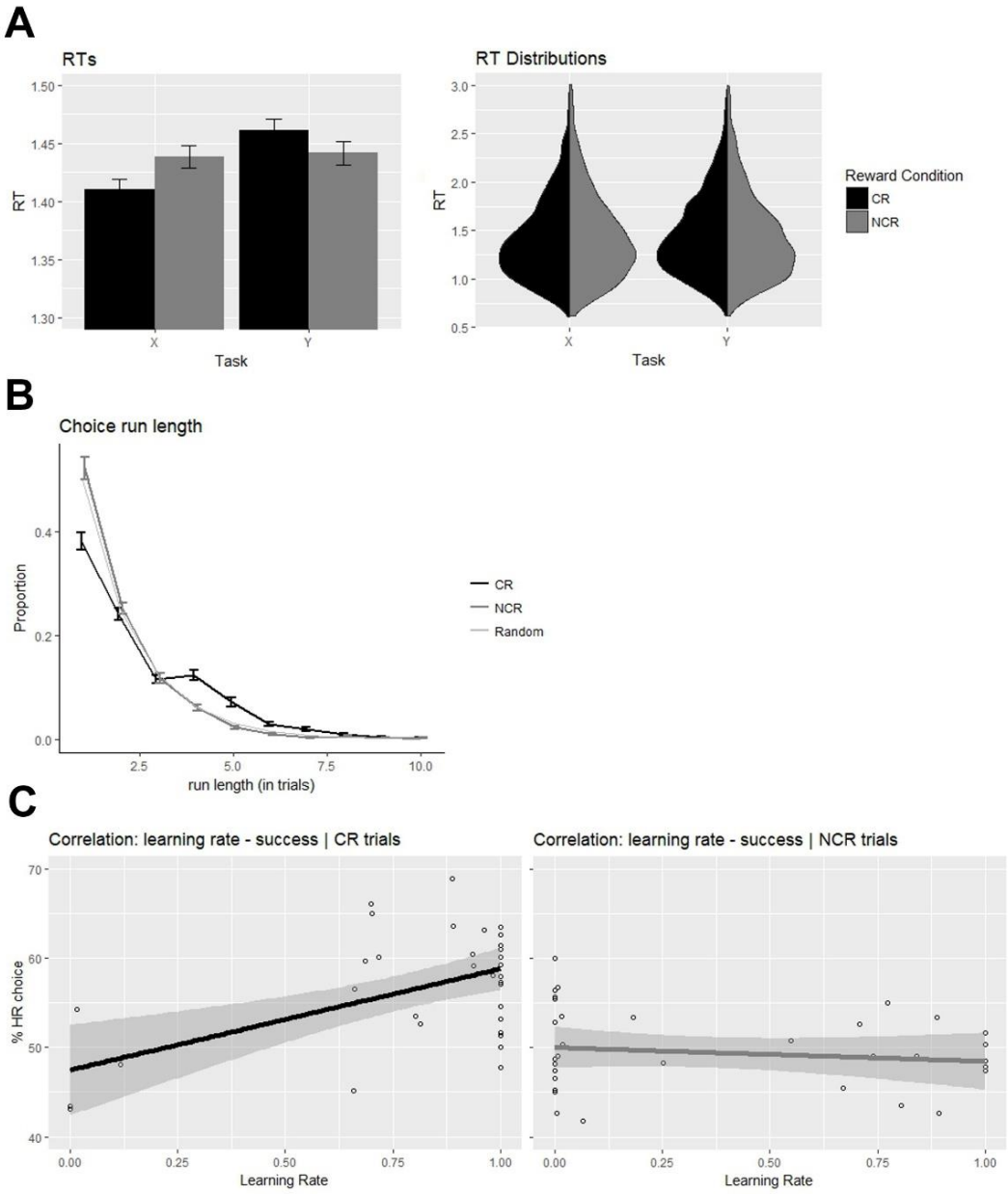

Figure 2. **Behavioral Results. A.** Reaction Times (RT). The bar graph depicts the average reaction times for each combination of task and reward condition. Contingent (CR) trials are shown in black, non-contingent (NCR) trials are shown in grey. The violin plot depicts the RT distributions of the same data. **B.** Choice run length. This plot depicts the distribution of run lengths (the number of consecutive trials in the same task). Data from CR trials is shown in black, data from NCR trials is shown in grey. The expected distribution if choices were completely random is depicted in light grey. All error bars depict the SEM. **C.** Correlation of learning rate and success. Learning rates were extracted form a fitted RL model. Success was measured as % HR task choices. In CR trial, subjects who learned the changing reward contingencies quickly, were

more successful. In NCR, no such correlation was observed. Each dot represents one subject, and linear functions were fitted to the data (lines). Further information on correlations between performance and additional questionnaire measures can be found in Supplementary Figure 1.

Behavioral results

We first assessed the effects of tasks (X, Y) and reward condition (CR, NCR) on error rates and reaction times (RT). The average error rate across all subjects was 5.89% (SEM = 0.74%). Thus, subjects were able to perform the task accurately. There was no evidence for an effect of reward condition on error rates (Bayes Factor (BF10) = 0.88, $t(34) = 1.96$, $p = 0.06$). Error trials were removed from all further analyses. A repeated-measures ANOVA on the reaction times (RT) including the factors task and reward condition revealed no main effect of reward (BF01 = 31.95, $F(1,34) = 0.38$, $p = 0.53$, Figure 2 A). This is likely due to the fact that subjects had a long time to prepare the execution of the task, which minimized potential contingency-related differences in RTs. There was a strong main effect of task however (BF10 > 150, $F(1,34) = 3.78$, $p = 0.05$), with task X (RT_X = 1415ms, SEM = 29ms) being faster than task Y (RT_Y = 1467ms, SEM = 35ms). Please note, that this cannot be simply due to a difficulty difference between the two S-R-mappings called task X and task Y, as the specific S-R-mappings were counter-balanced across subjects. Given the long delay phase, subjects should have had enough time to prepare both tasks well, and we were somewhat surprised to see this RT difference. This results might reflect the encoding sequence in the learning phase. Subjects might have learned the S-R-mapping labelled X first, and then learned the S-R-mapping labelled Y second. If the second task is mainly encoded by how it differs from the first, this might lead to a RT difference (see also Lien et al., 2005). There was no evidence for an interaction between task and reward (BF10 = 0.26, $F(1,34) = 6.63$, $p = 0.01$).

We then assessed whether subjects showed choice biases towards one of the two tasks, which might indicate stable preferences for specific tasks and might in turn affect fMRI analyses (see below). In order to quantify any potential choice biases, we computed the percentage of task X choices for both reward

conditions separately. Subjects chose task X in 52.14% (SEM = 1.44%) of the CR trials, and 52.29% (1.72%) of the NCR trials. These values did not differ from 50% in the CR condition (BF10 = 0.48, t(34) = 1.47, p = 0.14), and NCR condition (BF10 = 0.40, t(34) = 1.32, p = 0.19). There was also no difference between the two reward conditions (BF01 = 5.45, t(34) = 0.14, p = 0.88), indicating that subjects did not exhibit strong choice biases in this experiment.

Next, we measured subjects' success in solving the reversal learning task presented in CR trials, by computing the percentage of high-reward (HR) task choices for each subject. If they were unable to learn which of the two tasks was the HR task, this value should be 50%. Higher values indicate increasing success in performing the reversal learning task. We hypothesized that subjects chose HR tasks more often in CR, as compared to NCR trials. Subjects chose the HR task in 56.40% (SEM = 1.15%) of the CR trials, which was above chance level (BF10 >150, t(34) = 5.56, p < 0.001). They chose the HR task in 49.47% (SEM = 0.84%) of the NCR trials, which did not differ from the chance level (BF01 = 4.59, t(34) = 0.62, p = 0.53). Importantly, we found strong evidence for our hypothesis that subjects chose HR tasks more often in the CR, than in the NCR condition (BF10 > 150, t(34) = 5.44, p < 0.001). These findings demonstrate that subjects indeed chose tasks strategically in the CR condition, in order to maximize their reward outcome.

We then described the learning process in the CR trials in more details by fitting a reinforcement learning (RL) model (Sutton and Barto, 1990, see Materials and Methods for more details) to the choice data of each subject, and extracting the estimated learning rate (α). We expected subjects to show high learning rates in CR trials, reflecting the fact that subjects frequently needed to update which of the two tasks yielded higher reward outcomes. We compared fitted models in both CR and NCR trials to a null model, in which the learning rate was fixed to 0, assuming that subjects never learned about the reward contingencies in this experiment. Model fit was assessed using the AIC and BIC (Burnham and Anderson, 2004). As expected, the RL model provided a better fit to the data than the null model in both CR trials (AIC_{RL_CR}=129.97, AIC_{NULL_CR}=159.54, BIC_{RL_CR}=132.71, BIC_{NULL_CR}=159.54), as well as NCR trials

564 (AIC_{RL_NCR}=158.70, AIC_{NULL_NCR}=158.90, BIC_{RL_NCR}=132.71, BIC_{NULL_NCR}=158.90). Given that reward
565 contingencies changed frequently in the CR trials, we expected learning rates to be higher in CR than in
566 NCR trials. We found strong evidence in favor of this hypothesis (α_{CR}: mean = .78, median = .96, sd = .33,
567 min/max = <.001/1; α_{NCR}: mean = .36, median = .06, sd = .41, min/max = <.001/1; BF10 > 150, t(34) = 4.63,
568 p < 0.001). We then correlated estimated learning rates with successful task performance (% HR task
569 choices), again using a Bayesian framework for correlation estimation (using *bayes.cor.test* form the
570 BayesianFirstAid package in R). Specifically, we estimated the probability of the correlation being above 0
571 (p(r>0)), and also estimated 95% credible intervals (95% CI), which indicates the range of values within
572 which the correlation falls with a 95% probability. If this interval did not include 0, we interpreted the
573 correlation as either positive or negative. The estimated learning rate in CR trials was indeed correlated
574 with successful task performance (% HR task choices), r = .44 (95% CI = [.026, .74], p(r>0) = .97, Figure 2
575 C), linking our computational modelling more closely to behavior. As a control analysis, we also correlated
576 learning rate in NCR with proportion of HR task choices in NCR trials. As expected, we found no correlation,
577 r=-.12 (95% CI = [-.46, .21], p(r>0) = .21). Classically estimated correlations confirmed these results, r = .56,
578 p < 0.001, and r = -.12, p = 0.46, respectively. These results indicate that successful subjects were able to
579 learn about changing reward contingencies more quickly, and also demonstrate that subjects treated both
580 reward conditions differently.

581 Lastly, in NCR trials we expected subjects to choose tasks randomly, as their choices had no effect on
582 reward outcomes (see Materials and Methods for more details). In order to test this, we computed the
583 run length for each subject, i.e. the average number of consecutive trials in the same task (Arrington and
584 Logan, 2004). The average run length was then compared to the expected theoretical distribution if
585 choices were fully random (Figure 2 B). The average run length in NCR trials was 1.95 trials (SEM = 0.07
586 trials), which did not differ from the expected 'random-choice' run length (BF01 = 4.85, t(34) = 0.52, p =
587 0.60). Subjects in this experiment thus did not exhibit repetition bias, which has been reported previously

588 for free-choice tasks (Arrington and Logan, 2004). The average run length in CR trials was 2.54 trials (SEM
589 = 0.08 trials), which was longer than in NCR trials (BF10 >150, $t(34) = 5.91$, $p < 0.001$), demonstrating that
590 subjects stayed longer in the same task. This is a viable strategy in the reversal-learning task they
591 performed. Once they identified which was the HR task, repeatedly performing that task maximized
592 reward outcomes.

593 Reward-related brain activity

594 Multivariate decoding of reward outcome values

595 One of our main goals was to assess whether reward contingency affects valuation processes in the brain.
596 In a first analysis, we aimed to extend previous findings demonstrating an effect of reward contingency
597 on the processing of its hedonic value (Elliott et al., 2004). For this purpose, identified brain regions
598 encoding outcome values (high vs low) at the time of feedback presentation. We found an extensive
599 network to encode outcome values including subcortical brain regions, as well as large parts of the
600 prefrontal and parietal cortex (Figure 3 A). Please note that this contrast might not *only* capture specific
601 reward value signals, it might also reflect effects caused by differences in reward outcomes, like attention
602 or motor preparation. We explicitly assessed whether reaction times affected outcome coding (see Todd
603 et al., 2013), and found no effect (Figure 3-1). Subsequently, we assessed whether these outcome signals
604 were modulated by reward contingency, hypothesizing that contingent rewards showed stronger
605 decoding results than non-contingent rewards. For this purpose, we repeated the decoding analysis
606 described above, now separately for CR and NCR trials, respectively. The two resulting accuracy maps
607 were entered into a within-subjects ANOVA, and a contrast was computed identifying brain regions with
608 higher accuracies in CR than in NCR trials. Using small-volume correction ($p < 0.001$ uncorrected, $p < 0.05$
609 FWE corrected), we assessed which of the brain regions identified in the *baseline* analysis also showed
610 stronger value coding for contingent rewards. We found the striatum, bilateral lateral PFC, dACC, anterior

medial PFC, and IPS to show stronger reward value coding for contingent rewards, as compared to non-contingent rewards. In a last step, we directly assessed whether there were brain regions that encoded reward values in a contingency-invariant fashion, using a cross-classification approach. Here, we trained a classifier to distinguish high from low rewards only on CR trials, and then tested its performance on NCR trials, and vice versa. This allowed us to identify brain regions in which outcome values are encoded invariantly across the two contingency conditions, i.e. where neural patterns do not differ across contingency conditions (Kaplan et al., 2015). We found the striatum, lateral and medial PFC, dACC, and IPS to encode rewards in a contingency invariant form. This pattern of results suggests that the neural code for different reward values did not change across contingency conditions, yet value signals were still stronger in CR than in NCR trials. This is compatible with an increased gain or amplification of value representations through contingency (Figure 3 B), where representations do not change but become more separable in neural state space (see Waskom et al., 2014 for a similar argument).

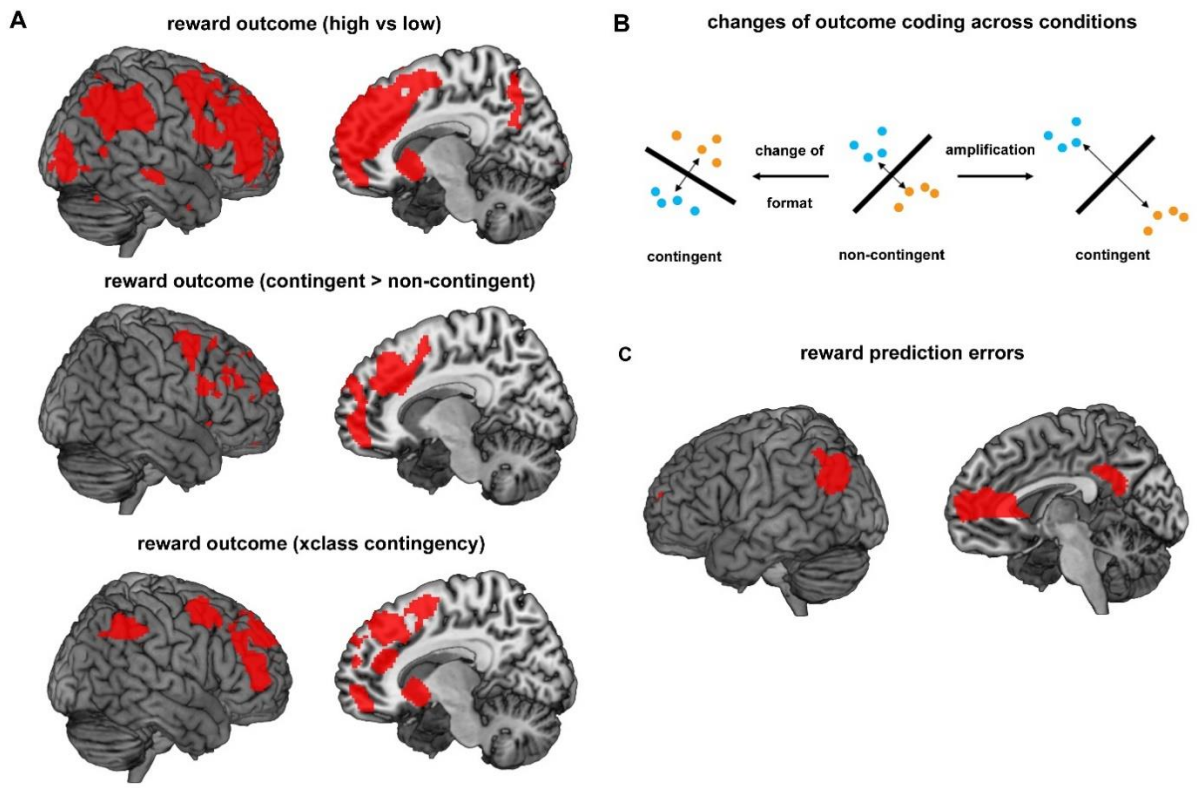

Figure 3: Reward-related brain activity. A. Multivariate decoding of reward outcome value. Above: baseline decoding. Depicted are regions that encoded the value of reward outcomes (high vs. low). The regions identified were used as masks for the following analyses. Results are displayed at $p < 0.05$ (FWE corrected). Middle: regions with a stronger coding of reward value in contingent (CR) than in non-contingent (NCR) trials. Below: regions encoding reward values in similar formats in both contingency conditions, as tested using a cross-classification (xclass) analysis. We also repeated this analysis, explicitly controlling for the effect of reaction times, and results can be found in Supplementary Figure 2. **B.** Amplification vs change of format of neural coding. Most regions identified in A showed both stronger decoding in CR trials, and similar formats across both contingency conditions. This is compatible with an amplification or gain increase of neural codes. In the middle, a hypothetical example of a pattern decoding is depicted. High reward trials are depicted as blue, low reward trials as orange dots. The classifier fits a decision boundary to separate the two distributions. If this code changes between the two contingency conditions (left), decoding is still possible at similar accuracy levels as before, but a classifier trained on NCR trials will be unsuccessful in classifying CR trials. If this code is amplified in the CR condition however (right), the same classifier can will be successful in both conditions. Accuracies increase, as the two distributions become more separable. **C.** Brain regions correlating with reward prediction error signals (in both CR and NCR trials).

Learning signals: Reward prediction errors

In the previous analysis, we assessed which brain regions directly encoded different reward outcomes in individual trials. We now turn to identifying brain regions supporting reward-based learning processes across multiple trials. We used the fitted RL models (see above) to extract trial-by-trials reward prediction errors (RPEs), which signal the need to adapt one's behavior (O'Reilly et al., 2013). Following a model-based neuroscience approach (Forstmann and Wagenmakers, 2015), we identified brain regions in which activity correlated with RPEs. These learning signals should be strongest at the time of decision-making (in our case the reward feedback presentation, see Materials and Methods for more details), and we found the left parietal cortex and anterior medial PFC to correlate with RPEs in CR trials (Figure 3 C). In NCR trials, we found anterior cingulate and anterior medial prefrontal cortex to encode RPEs. We statistically assessed the difference between these two results, using a within-subjects ANOVA with the factor 'model' (2 levels). We found no significant differences ($p < 0.001$ (uncorrected) at the voxel level, $p < 0.05$ (FWE corrected) at the cluster level), and thus decided to combine both conditions to increase statistical power. Running the same analysis over all trials (CR and NCR) again revealed the left parietal cortex (overlapping with the region identified in Analysis 1), ACC and anterior medial PFC, but also the precuneus. These regions thus signal discrepancies between expected and received rewards during feedback presentation, indicating the need to adapt behavior in the subsequent trial.

These brain regions could either signal general surprise, as RPEs are the difference between expected and received rewards (O'Reilly et al., 2013). They could also signal the need to update an internal model of our environment. Our findings are more in line with the former option. Any region signaling the need to update the internal model of the environment should be specifically involved only in CR trials (where updating is required), and not in NCR trials (where updating is not needed). In order to test this, we identified subjects that only showed high learning rates in CR and low learning rates in NCR trials (n=19). For these subjects, prediction errors only signaled the need to update their internal model. Results

668 showed that for this subset of subjects, only the anterior medial PFC correlated with RPEs ($p < 0.001$
669 uncorrected at the voxel, and $p < 0.05$ FWE corrected at the cluster level). This seems to suggest that the
670 anterior medial PFC was involved in model updating, while the left parietal cortex and precuneus signaled
671 general surprise. Given that the sample size was considerably smaller in this analysis, results should be
672 interpreted with caution however.

673 Multivariate decoding of tasks

674 *Baseline decoding analysis*: The previous analysis demonstrated that reward contingency indeed affected
675 the neural processing of the hedonic value of reward outcomes, and possibly also related learning signals.
676 In the following analysis we assessed whether these effects propagated to the implementation of chosen
677 behavior, i.e. the coding of chosen tasks as well. For this purpose, we first estimated a GLM modelling
678 task-related neural activity during the maintenance of chosen tasks, from the onset of the 'choose' cue to
679 the onset of the task execution screen. (see Materials and Methods for more details, and Haynes et al.
680 (2007) for a similar approach). During this time, subjects needed to maintain their intention to perform
681 one of the two tasks. We performed a searchlight decoding analysis contrasting task X and task Y,
682 combining both CR and NCR trials in order to maximize the power to detect any brain regions containing
683 task information (see Loose et al., 2017 for a similar approach). Please note that during this time subjects
684 cannot prepare specific motor responses yet, but they can use this time to retrieve the current S-R-
685 mapping. We found two brain regions to contain task information, the left posterior parietal cortex (mean
686 accuracy = 4.61%, SEM = 0.65%), spanning over the midline into the right parietal cortex, and the right
687 anterior middle frontal gyrus (aMFG, mean accuracy = 4.66%, SEM = 0.89%, see Figure 4 A, Table 1).
688 Interestingly, the parietal cluster identified in this analysis partly overlapped with the parietal cluster
689 found to encode reward prediction errors in the previous analysis, suggesting that the left parietal cortex
690 is involved in both reward-learning and task processing.

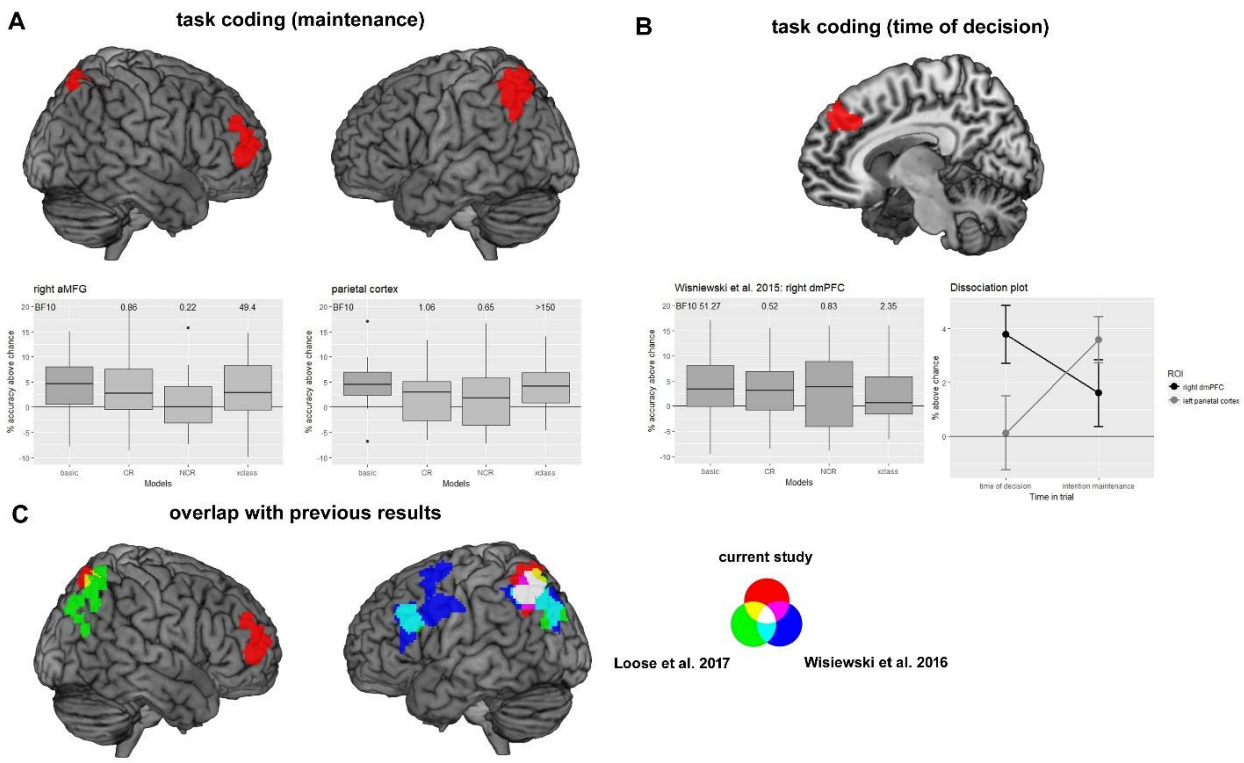

Figure 4: **Task coding**. **A.** Task coding during maintenance. Results from the baseline decoding analysis are depicted above. Two clusters passed the significance threshold, one in the parietal cortex, and one in the right anterior MFG. These two clusters were then used as ROIs, and accuracies were extracted for the contingent (CR), non-contingent (NCR), and cross-classification (xclass) task decoding analyses. Results can be seen below. Above the boxplots, Bayes factors (BF10) of a t-test vs. chance level are shown. Please note, that we do not report BF10 for the baseline analysis, as this analysis was used to define the ROIs, and running additional statistical tests on this data would constitute double dipping. **B.** Task coding at the time of decision-making. Above the ROI in the right dmPFC used in this analysis from Wisniewski et al. (2015) is depicted. This study demonstrated that the right dmPFC encodes tasks at the time of decision-making. The box plot depicts results from our data in this ROI, for all four analyses performed (baseline, CR, NCR, xclass). We largely replicate these previous findings. The dissociation plot depicts a double dissociation between two ROIs (right dmPFC, as defined using data from Wisniewski et al., 2015, and the left parietal cortex, as defined using data from Wisniewski et al., 2016), and two time points in the trial (time of decision-making, maintenance). It can be seen that the dmPFC only encodes tasks at the time of decision-making, while the left parietal cortex only encodes tasks during the maintenance phase. All error bars represent SEM. **C.** Overlap with previous results. Results from the current study (red) are overlain on previous findings from Wisniewski et al. 2016 (blue), and Loose et al. 2017 (green). All results are based on task decoding analyses (searchlight decoding, radius = 3 voxels, C = 1, chance level = 50%), albeit with different specific tasks being contrasted in each study. Despite this fact, all three studies find task information around the intraparietal sulcus. Findings in the PFC are less consistent. We further assessed task information encoded throughout the multiple-demand network, results can be found in Supplementary Figure 3.

714 **Table 1: Baseline task decoding**

				MNI coordinates (peak)		
Brain region	**Side**	**Cluster size**	**Mean accuracy (SEM)**	**X**	**Y**	**Z**
parietal cortex	Bilateral	2427	4.61% (0.65%)	-10	-60	60
anterior MFG	Right	955	4.66% (0.89%)	32	58	18

715 Results are shown for a statistical threshold of p<0.001 (uncorrected) at the voxel level and p<0.05 (FWE
716 corrected) at the cluster level.

717

718 *Differences in task coding*: In a next step, we assessed whether tasks were encoded with a higher accuracy
719 in CR, than in NCR trials, similar to what we found for reward outcomes. Previous research demonstrated
720 higher decoding accuracies in rewarded, as compared to non-rewarded tasks (Etzel et al., 2016). We built
721 functional ROIs from the two regions identified in the baseline analysis, and extracted the average
722 accuracy values for the task decoding analyses performed on CR trials only, and NCR trials only. Please
723 note that these two analyses use only half as many trials as the baseline analysis, and the signal-to-noise-
724 ratio can be expected to be lower. We found no task information in the parietal cortex in these two
725 analyses (CR: 1.29%, SEM = 0.91%, BF10 = 1.06, t(34) = 1.59, p = 0.06; NCR: 1.73%, SEM = 1.44%, BF10 =
726 0.64, t(34) = 1.23, p = 0.11), and found no evidence for stronger task coding in CR than in NCR trials (BF10
727 = 0.16, t(34) = 0.09, p = 0.53). A similar pattern of results was found in the right aMFG (CR: 1.79%, SEM =
728 1.37%, BF10 = 0.85, t(34) = 1.44, p = 0.07; NCR: 0.48%, SEM = 1.35%, BF10 = 0.22, t(34) = 0.25, p = 0.40;
729 CR > NCR: BF10 = 0.40, t(34) = 0.84, p = 0.20). Thus, we find no evidence for an effect of reward
730 contingency on task representations, despite the fact that behavior clearly differed between the two
731 reward conditions, and that contingency has been found to modulate the coding of reward outcomes. In
732 order to assess whether the lack of evidence for differences in task coding might stem from a lack in

statistical power, we performed an additional control analysis. We again performed two separate task decoding analysis, only using high reward and low reward trials (instead of CR and NCR trials), respectively. We then tested whether decoding accuracies differed between these two conditions. Importantly, this analysis has a similar statistical power, as the same number of trials is used. And indeed, we found task coding to differ between these two conditions even at the whole brain level ($p < 0.001$ uncorrected at the voxel, and $p < 0.05$ FWE corrected at the cluster level). Please note that this comparison might confound effects of reward value with attentional processes. Nevertheless, this shows that our analysis approach is able to identify differences in task coding in this dataset, although it fails to do so for our reward contingency manipulation.

Similarities in task coding: We also directly tested whether task representations were invariant across the two reward conditions, using a cross-classification approach. We trained a classifier to distinguish tasks in CR trials, and tested its performance in NCR trials, and vice versa. In this analysis, accuracies can only be above chance if task coding is invariant across both conditions. Results indicate than both the parietal cortex (4.03%, SEM = 0.76%, BF10 > 150), as well as the right aMFG (3.71%, SEM = 1.16%, BF10 = 49.39) show this type of contingency-invariant task coding. We further tested whether accuracies in the cross-classification differed from the baseline accuracies, finding moderate evidence for an absence of any differences (parietal cortex BF01 = 4.34, $t(34) = 0.71$, $p = 0.47$, aMFG BF01 = 3.94, $t(34) = 0.84$, $p = 0.40$). These results thus show that the parietal cortex and aMFG encode tasks using a general, reward-contingency-invariant format.

ROI analyses and replications: We also tested for task information in several a-priori ROIs, taken from two previous experiments (Loose et al. 2017, Wisniewski et al. 2016), which tested for effects of cognitive control, and free choice on task coding, respectively. Both previous studies found the left parietal cortex to be involved in context-invariant task coding, and we thus set out to replicate these previous results here. We extracted the ROIs reported in these two studies, and extracted decoding accuracies in each of

these ROIs, for all 4 analyses performed here (baseline, CR, NCR, xclass). We were able to replicate Loose and colleagues' left parietal results (baseline BF10 = 133.69, t(34) = 3.89, p < 0.001; CR BF10 = 0.68, t(34) = 1.23, p = 0.10; NCR BF10 = 0.54, t(34) = 1.11, p = 0.13; xclass BF10 = 33.17, t(34) = 3.33, p = 0.001). Although somewhat weaker, we also replicated their right parietal results (baseline BF10 = 8.49, t(34) = 2.72, p = 0.004; CR BF10 = 0.77, t(34) = 1.37, p = 0.08; NCR BF10 = 0.14, t(34) = 0.28, p = 0.61; xclass BF10 = 8.10, t(34) = 2.70, p = 0.005). However, we were unable to detect task information in left PFC (baseline BF10 = 0.49, t(34) = 1.03, p = 0.15; CR BF10 = 0.21, t(34) = 0.23, p = 0.40; NCR BF10 = 0.44, t(34) = 0.93, p = 0.17; xclass BF10 = 0.29, t(34) = 0.54, p = 0.29), which is in line with the original paper, where PFC findings were also somewhat less robust. Additionally, we were able to replicate Wisniewski and colleagues' left parietal finding (baseline BF10 = >150, t(34) = 4.20, p < 0.001; CR BF10 = 0.80, t(34) = 1.40, p = 0.08; NCR BF10 = 0.47, t(34) = 1.00, p = 0.16; xclass BF10 = 87.28, t(34) = 3.72, p < 0.001), as well as left BA8 (baseline BF10 = 9.3, t(34) = 2.77, p = 0.004; CR BF10 = 0.39, t(34) = 0.83, p = 0.20; NCR BF10 = 0.36, t(34) = 0.76, p = 0.22; xclass BF10 = 3.09, t(34) = 2.22, p = 0.16), but not the left PFC (baseline BF10 = 0.59, t(34) = 1.17, p = 0.12; CR BF10 = 0.37, t(34) = 0.78, p = 0.21; NCR BF10 = 0.16, t(34) = 0.15, p = 0.56; xclass BF10 = 0.38, t(34) = 0.81, p = 0.21). Thus, three studies with similar overall designs but considerable differences in the specific tasks used consistently find invariant task coding in the parietal, but not in the prefrontal cortex.

Furthermore, Wisniewski et al. 2015 found task information at the time of decision-making in the right dorso-medial PFC (Figure 4 B). In order to replicate this finding, we repeated all 4 task decoding analysis, only looking at the time of decision-making instead of intention maintenance (which was the reward feedback presentation in this experiment, see Materials and Methods for more details). The right dmPFC, as identified by Wisniewski and colleagues, was found to encode tasks also in the current study (baseline 3.76%, SEM = 1.07%, BF10 = 51.27, t(34) = 3.51, p < 0.001, Figure 4 B). This was despite the fact that there were considerable differences in the overall experimental design of these two studies (e.g. 2 class vs. 3 class decoding, changing reward outcomes vs. changing task difficulty). We found anecdotal evidence for

781 contingency-invariant task coding in this region (xclass 2.03%, SEM = 0.98%, BF10 = 2.35, t(34) = 2.07, p =
782 0.02), although the baseline and xclass analyses did not differ (BF10 = 1.64, t(34) = 1.63, p = 0.11).
783 Interestingly, the dmPFC was also found to encode reward outcome values, with its outcome signal being
784 amplified by our contingency manipulation (Figure 3 A). This region thus simultaneously encoded both
785 reward outcomes and the choices informed by these outcomes, highlighting its role in linking value to
786 intention processing in the brain. Additionally, we found a double dissociation in task coding between the
787 right dmPFC and left parietal cortex (Figure 4B), with the former only encoding tasks at the time of
788 decision-making, and the latter only encoding tasks during intention maintenance. Please note that due a
789 jittered inter-trial-interval, the decision-time and intention maintenance could be investigated
790 independently. This dissociation was assessed statistically by performing an ANOVA on the accuracy
791 values, using the factors 'time in trial' (time of decision vs intention maintenance) and 'ROI' (right dmPFC
792 vs left parietal cortex). We found moderate evidence for a time x ROI interaction (BF10 = 5.39, F(1,34) =
793 10.49, p = 0.04). Furthermore, the right dmPFC only encoded tasks at the time of decision (BF10 = 51.27,
794 t(34) = 3.51, p < 0.001), but not during intention maintenance (BF10 = 0.68, t(34) = 1.28, p = 0.10). The left
795 parietal cortex only encoded tasks during intention maintenance (BF10 > 150, t(34) = 4.20, p < 0.001), but
796 not at time of decision (BF10 = 0.19, t(34) = 0.09, p = 0.46). This double dissociation thus suggests a
797 temporal order of task processing in the brain, with the medial PFC transiently encoding chosen tasks at
798 the time of decision-making, and the left parietal cortex then maintaining that information until the tasks
799 can be executed. Lastly, we also assessed task information throughout the multiple demand network
800 (Duncan, 2010; Woolgar et al., 2015), and found tasks to be encoded in a contingency-invariant format
801 (Figure 4-1).

802 *Control analyses*: In order to provide further support for our main results, we decided to perform a
803 number of additional control analyses. First, we controlled for potential effects of RTs on task decoding
804 results. It has been pointed out before, that task information in the brain can at least partly be explained

through RT effects (Todd et al., 2013). Although others have found no such effects (Woolgar et al., 2014), we decided to conservatively control for RT effects nonetheless, especially given that we found RT differences between tasks (see above). We thus repeated the task decoding analyses, only first regressing RT-related effects out of the data. We used the parietal and aMFG ROIs defined in the baseline analysis and tested whether task information was still present after controlling for potential RT effects. We still found the parietal cortex to encode tasks (4.61%, SEM = 0.65%, BF10 > 150, $t(34) = 6.99$, $p < 0.001$), and also found the task coding to be reward-invariant (4.03%, SEM = 0.76%, BF10 > 150, $t(34) = 5.24$, $p < 0.001$). The same was true for the aMFG (4.66%, SEM = 0.89%, BF10 > 150, $t(34) = 5.19$, $p < 0.001$; and 3.71%, SEM = 1.16%, BF10 = 23.38, $t(34) = 3.18$, $p = 0.001$; respectively). Results in the baseline and xclass analysis were equal in both regions, BFs10 >= 3.24, $ts(34) < 0.67$, $ps > 0.25$. These results thus mirror the main analysis above, showing that RT-related variance cannot explain task decoding results in our experiment.

Although overall error rates were low and choice biases were largely absent, it was still possible that individual subjects showed excessively high error rates or strong choice biases, affecting task decoding results. The influence of individual subjects should be relatively small given our large sample size, but we still repeated the main analyses, excluding subjects with excessively high error rates and excessively strong choice biases. Additionally, we excluded subjects in which regressors could not be estimated from a sufficient number of trials (see Materials and Methods for more details). Using these highly conservative exclusion criteria, we removed an additional 12 subjects from the sample, leading to a sample size of 23 subjects. Even though statistical power was considerably lower because of the smaller sample size, we were still able to detect task information in the parietal cortex (5.20%, SEM = 0.79%, BF10 >150, $t(22) = 6.54$, $p < 0.001$), which was again reward-invariant (3.81%, SEM = 0.96%, BF10 = 96.61, $t(22) = 3.93$, $p < 0.001$), and the same was true for the aMFG (5.03%, SEM = 1.09%, BF10 >150, $t(22) = 4.60$, $p < 0.001$, and

3.71%, SEM = 1.39%, BF10 = 7.34, $t(22) = 2.66$, $p = 0.006$, respectively). Therefore, neither error rates, nor choice biases can explain the reported task decoding results.

In order to validate the decoding procedure, we also extracted task decoding accuracies from a region not involved in performing this task, the primary auditory cortex. As expected, we found accuracies not to differ from chance level in this region (-0.36%, SEM = 0.93%, BF01 = 7.22, $t(34) = 0.38$, $p = 0.64$), showing that the task decoding analysis was not biased towards positive accuracy values. Lastly, we empirically estimated the chance level of our decoding analysis using permutation tests, in order to rule out a biased chance level. The estimated chance level was 49.98%, which did not differ from the theoretical chance level of 50% (BF01 > 150, $t(34999) = 0.41$, $p = 0.67$). Thus, comparing our decoding accuracies against a chance level of 50% was valid.

Discussion

Here, we investigated the effects of control over choice outcomes on outcome valuation and choice implementation. Subjects performed a probabilistic reward reversal learning task, in which they had control over the outcomes of their choices. They also performed a free choice task with non-contingent reward outcomes, in which outcomes were not under their direct control. Although we found reward contingency to modulate outcome valuation, we found no effects on choice implementation. Furthermore, we found two main brain regions to be crucial for encoding tasks and reward outcomes: the right dmPFC and the left parietal cortex (around the IPS). The dmPFC was found to encode chosen tasks at the time of decision-making, and simultaneously encoded reward outcome values, emphasizing its role in linking value-related with intentional control processes. While the parietal cortex encoded reward-prediction errors at the time of decision-making, it encoded chosen tasks during a subsequent maintenance phase. We found a double dissociation between both regions, with the dmPFC encoding tasks only at the time of decision-making, and the parietal cortex only during intention maintenance.

Control over choice outcomes affects outcome valuation but not choice implementation

Much previous research on the effects of reward motivation on cognition investigated the effects of reward prospect (Jimura et al., 2010; Dreisbach and Fischer, 2012). These findings demonstrated that positive reinforcement improves cognition, as compared to no reinforcement at all. However, an equally important and often overlooked property of reinforcement is the degree of control we have in reaching it. Sometimes, an action will cause on outcomes in a fairly clear way, other times, that link will be less close. Previous work on non-human primates has shown that the strength of such action-outcome contingencies modulates the neural processing of reward outcomes (Izquierdo et al., 2004; Chudasama et al., 2013). Our results show that this is also true in humans (see also Tricomi et al., 2004), and that neural representations of outcome values (and correlated processes) are amplified by reward contingency. Although somewhat weaker, evidence for reward learning signals points in the same direction. This is in line with predictions from gain-theories of motivation. It has been suggested that rewards increase the gain of subcortical dopaminergic neurons (Tobler et al., 2005), making them more sensitive to changes in rewards (see also Ikeda and Hikosaka, 2003; Thurley et al., 2008). We directly demonstrate such gain increases, in subcortical dopaminergic regions and beyond.

Importantly, in order for this value signal to lead to actual rewards, chosen behavior has to be implemented as intended first. One might thus expect contingency to lead to stronger task shielding and coding (Dreisbach and Wenke, 2011), as the costs of confusing both tasks are potentially high. However, we found no evidence for such effects. On the contrary, we found evidence for a similar or invariant coding of tasks across both contingency conditions. This finding informs current debates on the nature of task coding in the brain. On the one hand, some have argued for flexible task coding especially in the fronto-parietal cortex (Woolgar et al., 2015; Qiao et al., 2017), often based on the multiple-demand network theory (Duncan, 2010). This account predicts that task coding should be stronger when task demands are high (Woolgar et al., 2015), or when correct performance is rewarded (Etzel et al., 2016). Despite our

875 efforts to replicate these findings in our data-set, we found no evidence for an influence of reward
876 contingency on task coding. This was despite the fact that behavior differed between these conditions
877 and that value-related signals were affected by reward contingency. One might argue that our analysis
878 had insufficient statistical power to detect true effects, though we believe this to be unlikely. First, we
879 decided to have a relatively large sample size (n=35). Second, additional control analyses showed that
880 other analyses, matched for statistical power, do show significant results.

881 On the other hand, others have argued that the same task representations could be used in multiple
882 different situations (i.e. 'multiplexing' of task information), and that this allows us to flexibly react to novel
883 and changing demands (Botvinick and Cohen, 2014). Multiplexing predicts that task information should
884 be invariant across different contexts (Levine and Schwarzbach, 2017), which has been shown previously
885 (Zhang et al., 2013; Wisniewski et al., 2016; Loose et al., 2017). Here, we replicate and extend these
886 findings, by showing that tasks are encoded in an outcome-contingency-invariant format in frontal and
887 parietal brain regions, strengthening the idea of multiplexing of task information in the brain. One possible
888 alternative explanation for this finding might be that subjects were highly trained in performing the two
889 tasks, and were at their performance ceiling. This might make a modulation of task coding too small to
890 detect. Although we cannot fully exclude this interpretation, we want to point out that contingency did
891 have robust effects on behavior. Also, most related previous experiments trained their subjects, those
892 who found effects (Woolgar et al., 2015; Etzel et al., 2016) and those that did not (Wisniewski et al., 2016).
893 We thus believe this alternative explanation to be unlikely. Overall, our task decoding results are in line
894 with the idea of multiplexing of task information in the brain. Future research will have to test more
895 directly which environmental conditions lead to multiplexing of task information in the brain, and which
896 do not.

897 ## The roles of dmPFC and parietal cortex in value-related and task-related processes

898 The dmPFC is a key region for decision-making in dynamic environments. It is supports effort-based
899 foraging choices (Wisniewski et al., 2015b), and here we extend this finding by showing its involvement in
900 a different task with different outcomes (reward reversal learning). The dmPFC is important for cognitive
901 control, supporting rule and action selection (Rowe et al., 2008), working memory (Taylor et al., 2004),
902 and processing uncertainty (Volz et al., 2003). It has further been associated with valuation processes,
903 anticipating both positive and negative outcomes (Jensen et al., 2003; Knutson et al., 2003), and encoding
904 reward prediction errors (Vassena et al., 2014). In this experiment, we demonstrated that the dmPFC is
905 specifically involved in encoding tasks only at the time at which a choice is made, other regions later
906 maintain that choice outcome until it can be executed. We also demonstrated the dmPFC to encode
907 outcome values at the same time. Please note that we do not claim this value signal to only represent the
908 magnitude of reward outcomes, it might also represent related processes (e.g. attention). Nevertheless,
909 the cause of this effect are different outcome values, and this highlights the importance of dmPFC in
910 linking valuation to strategic decision-making, providing an explanation to how it might support goal-
911 directed behavior (Viard et al., 2011).

912 The second key region identified in this experiment was the left parietal cortex, especially around the IPS.
913 This brain region encodes prediction errors (Daw and Doya, 2006; Matsumoto et al., 2007; Katahira et al.,
914 2015), which might signal model updating (Behrens et al., 2007; Walton et al., 2007; Rutledge et al., 2010).
915 Alternatively, it has been suggested that the parietal cortex signals surprise, and does not reflect model
916 updating (O'Reilly et al., 2013). Our findings are more in line with surprise signaling, the only brain region
917 possibly involved in model updating in our experiment was the anterior medial PFC (see also (Braem et
918 al., 2013). The parietal cortex is also a key region for cognitive control (Ruge et al., 2009), and working
919 memory (Christophel et al., 2017). It is part of the multiple demand network (Duncan, 2010; Fedorenko
920 et al., 2013), a set of brain regions characterized by their high flexibility to adapt to changing demands.

921 Previous work on non-human primates demonstrated that the prefrontal cortex flexibly switches between
922 representing different control-related information within single trials (Sigala et al., 2008; Stokes et al.,
923 2013). Our results show that the parietal cortex in humans exhibits similar flexibility. It switches between
924 encoding control-related and value-related variables within single trials. This provides compelling
925 evidence for the flexibility of the parietal cortex in adapting to rapidly changing task demands.

926 Conclusion

927 In this experiment, we assessed whether controlling outcomes affects outcome valuation and choice
928 implementation in the brain. By comparing choices that are informed by expected outcomes as well as
929 choices that are not, we linked largely parallel research on 'free choice' (Libet et al., 1983) and value-
930 based decision-making (Hampton and O'Doherty, 2007), which has been long overdue. While we found
931 strong effects on outcome valuation, we found no such effects on choice implementation. Our results
932 further highlight the importance of both the dmPFC and parietal cortex in bridging valuation and executive
933 processes in the brain. Both regions have been involved in processing task choices and their reward
934 outcomes, flexibly switching between encoding value-related and task-related information.

References

Andraszewicz S, Scheibehenne B, Rieskamp J, Grasman R, Verhagen J, Wagenmakers E-J (2015) An Introduction to Bayesian Hypothesis Testing for Management Research. J Manag 41:521–543.

Arrington CM, Logan GD (2004) The cost of a voluntary task switch. Psychol Sci 15:610–615.

Bai Y, Katahira K, Ohira H (2014) Dual learning processes underlying human decision-making in reversal learning tasks: functional significance and evidence from the model fit to human behavior. Front Psychol 5 Available at: https://www.frontiersin.org/articles/10.3389/fpsyg.2014.00871/full [Accessed May 31, 2018].

Behrens TEJ, Woolrich MW, Walton ME, Rushworth MFS (2007) Learning the value of information in an uncertain world. Nat Neurosci 10:1214–1221.

Bhandari A, Gagne C, Badre D (2018) Just above Chance: Is It Harder to Decode Information from Human Prefrontal Cortex Blood Oxygenation Level-dependent Signals? J Cogn Neurosci:1–26.

Botvinick MM, Cohen JD (2014) The Computational and Neural Basis of Cognitive Control: Charted Territory and New Frontiers. Cogn Sci 38:1249–1285.

Braem S, King JA, Korb FM, Krebs RM, Notebaert W, Egner T (2013) Affective Modulation of Cognitive Control is Determined by Performance-Contingency and Mediated by Ventromedial Prefrontal and Cingulate Cortex. J Neurosci 33:16961–16970.

Bunge SA, Kahn I, Wallis JD, Miller EK, Wagner AD (2003) Neural Circuits Subserving the Retrieval and Maintenance of Abstract Rules. J Neurophysiol 90:3419–3428.

Burnham KP, Anderson DR (2004) Multimodel Inference: Understanding AIC and BIC in Model Selection. Sociol Methods Res 33:261–304.

Cacioppo JT, Petty RE, Chuan Feng Kao (1984) The Efficient Assessment of Need for Cognition. J Pers Assess 48:306.

Carver CS, White TL (1994) Behavioral inhibition, behavioral activation, and affective responses to impending reward and punishment: the BIS/BAS scales. J Pers Soc Psychol 67:319.

Christophel TB, Klink PC, Spitzer B, Roelfsema PR, Haynes J-D (2017) The Distributed Nature of Working Memory. Trends Cogn Sci 21:111–124.

Chudasama Y, Daniels TE, Gorrin DP, Rhodes SEV, Rudebeck PH, Murray EA (2013) The Role of the Anterior Cingulate Cortex in Choices based on Reward Value and Reward Contingency. Cereb Cortex 23:2884–2898.

Collins AGE, Ciullo B, Frank MJ, Badre D (2017) Working Memory Load Strengthens Reward Prediction Errors. J Neurosci 37:4332–4342.

967 Cox DD, Savoy RL (2003) Functional magnetic resonance imaging (fMRI) “brain reading”: detecting and
968 classifying distributed patterns of fMRI activity in human visual cortex. NeuroImage 19:261–270.

969 Daw ND, Doya K (2006) The computational neurobiology of learning and reward. Curr Opin Neurobiol
970 16:199–204.

971 Daw ND, Gershman SJ, Seymour B, Dayan P, Dolan RJ (2011) Model-Based Influences on Humans’
972 Choices and Striatal Prediction Errors. Neuron 69:1204–1215.

973 Domenech P, Redouté J, Koechlin E, Dreher J-C (2018) The Neuro-Computational Architecture of Value-
974 Based Selection in the Human Brain. Cereb Cortex 28:585–601.

975 Doya K (2008) Modulators of decision making. Nat Neurosci 11:410–416.

976 Dreisbach G, Fischer R (2012) The role of affect and reward in the conflict-triggered adjustment of
977 cognitive control. Front Hum Neurosci 6 Available at:
978 http://www.ncbi.nlm.nih.gov/pmc/articles/PMC3533233/ [Accessed October 30, 2014].

979 Dreisbach G, Wenke D (2011) The shielding function of task sets and its relaxation during task switching.
980 J Exp Psychol Learn Mem Cogn 37:1540–1546.

981 Duncan J (2010) The multiple-demand (MD) system of the primate brain: mental programs for intelligent
982 behaviour. Trends Cogn Sci 14:172–179.

983 Eklund A, Nichols TE, Knutsson H (2016) Cluster failure: Why fMRI inferences for spatial extent have
984 inflated false-positive rates. Proc Natl Acad Sci 113:7900–7905.

985 Elliott R, Newman JL, Longe OA, William Deakin JF (2004) Instrumental responding for rewards is
986 associated with enhanced neuronal response in subcortical reward systems. NeuroImage
987 21:984–990.

988 Etzel JA, Cole MW, Zacks JM, Kay KN, Braver TS (2016) Reward Motivation Enhances Task Coding in
989 Frontoparietal Cortex. Cereb Cortex 26:1647–1659.

990 Fedorenko E, Duncan J, Kanwisher N (2013) Broad domain generality in focal regions of frontal and
991 parietal cortex. Proc Natl Acad Sci 110:16616–16621.

992 Forstmann BU, Wagenmakers E-J (2015) An Introduction to Model-Based Cognitive Neuroscience.
993 Springer.

994 Friston KJ, Holmes AP, Worsley KJ, Poline J-P, Frith CD, Frackowiak RS (1994) Statistical parametric maps
995 in functional imaging: a general linear approach. Hum Brain Mapp 2:189–210.

996 Gilbert SJ (2011) Decoding the Content of Delayed Intentions. J Neurosci 31:2888–2894.

997 Hampton AN, O’Doherty JP (2007) Decoding the neural substrates of reward-related decision making
998 with functional MRI. Proc Natl Acad Sci 104:1377–1382.

999 Haxby JV (2012) Multivariate pattern analysis of fMRI: The early beginnings. NeuroImage 62:852–855.

Haynes J-D (2015) A Primer on Pattern-Based Approaches to fMRI: Principles, Pitfalls, and Perspectives. Neuron 87:257–270.

Haynes J-D, Sakai K, Rees G, Gilbert SJ, Frith C, Passingham RE (2007) Reading Hidden Intentions in the Human Brain. Curr Biol 17:323–328.

Hebart MN, Görgen K, Haynes J-D (2014) The Decoding Toolbox (TDT): A versatile software package for multivariate analyses of functional imaging data. Front Neuroinformatics 8:88.

Ikeda T, Hikosaka O (2003) Reward-Dependent Gain and Bias of Visual Responses in Primate Superior Colliculus. Neuron 39:693–700.

Izquierdo A, Suda RK, Murray EA (2004) Bilateral Orbital Prefrontal Cortex Lesions in Rhesus Monkeys Disrupt Choices Guided by Both Reward Value and Reward Contingency. J Neurosci 24:7540–7548.

Jensen J, McIntosh AR, Crawley AP, Mikulis DJ, Remington G, Kapur S (2003) Direct Activation of the Ventral Striatum in Anticipation of Aversive Stimuli. Neuron 40:1251–1257.

Jimura K, Locke HS, Braver TS (2010) Prefrontal cortex mediation of cognitive enhancement in rewarding motivational contexts. Proc Natl Acad Sci 107:8871–8876.

Kahnt T, Park SQ, Haynes J-D, Tobler PN (2014) Disentangling neural representations of value and salience in the human brain. Proc Natl Acad Sci 111:5000–5005.

Kamitani Y, Tong F (2005) Decoding the visual and subjective contents of the human brain. Nat Neurosci 8:679–685.

Kaplan JT, Man K, Greening SG (2015) Multivariate cross-classification: applying machine learning techniques to characterize abstraction in neural representations. Front Hum Neurosci 9 Available at: http://www.ncbi.nlm.nih.gov/pmc/articles/PMC4373279/ [Accessed December 10, 2015].

Katahira K, Matsuda Y-T, Fujimura T, Ueno K, Asamizuya T, Suzuki C, Cheng K, Okanoya K, Okada M (2015) Neural basis of decision making guided by emotional outcomes. J Neurophysiol 113:3056–3068.

Knutson B, Fong GW, Bennett SM, Adams CM, Hommer D (2003) A region of mesial prefrontal cortex tracks monetarily rewarding outcomes: characterization with rapid event-related fMRI. NeuroImage 18:263–272.

Kriegeskorte N, Goebel R, Bandettini P (2006) Information-based functional brain mapping. Proc Natl Acad Sci 103:3863–3868.

Levine SM, Schwarzbach J (2017) Decoding of auditory and tactile perceptual decisions in parietal cortex. NeuroImage 162:297–305.

1033 Libet B, Gleason CA, Wright EW, Pearl DK (1983) Time of conscious intention to act in relation to onset of
1034 cerebral activity (readiness-potential) the unconscious initiation of a freely voluntary act. Brain
1035 106:623–642.

1036 Lien M-C, Ruthruff E, Remington RW, Johnston JC (2005) On the limits of advance preparation for a task
1037 switch: do people prepare all the task some of the time or some of the task all the time? J Exp
1038 Psychol Hum Percept Perform 31:299–315.

1039 Loose LS, Wisniewski D, Rusconi M, Goschke T, Haynes J-D (2017) Switch-Independent Task
1040 Representations in Frontal and Parietal Cortex. J Neurosci 37:8033–8042.

1041 Matsumoto M, Matsumoto K, Abe H, Tanaka K (2007) Medial prefrontal cell activity signaling prediction
1042 errors of action values. Nat Neurosci 10:647–656.

1043 Mertens G, De Houwer J (2016) Potentiation of the startle reflex is in line with contingency reversal
1044 instructions rather than the conditioning history. Biol Psychol 113:91–99.

1045 Mitchell TM, Hutchinson R, Niculescu RS, Pereira F, Wang X, Just M, Newman S (2004) Learning to
1046 decode cognitive states from brain images. Mach Learn 57:145–175.

1047 O'Doherty JP, Hampton A, Kim H (2007) Model-Based fMRI and Its Application to Reward Learning and
1048 Decision Making. Ann N Y Acad Sci 1104:35–53.

1049 O'Reilly JX, Schüffelgen U, Cuell SF, Behrens TEJ, Mars RB, Rushworth MFS (2013) Dissociable effects of
1050 surprise and model update in parietal and anterior cingulate cortex. Proc Natl Acad Sci
1051 110:E3660–E3669.

1052 Patton JH, Stanford MS, Barratt ES (1995) Factor structure of the Barratt impulsiveness scale. J Clin
1053 Psychol 51:768–774.

1054 Peirce JW (2007) PsychoPy—Psychophysics software in Python. J Neurosci Methods 162:8–13.

1055 Pessiglione M, Seymour B, Flandin G, Dolan RJ, Frith CD (2006) Dopamine-dependent prediction errors
1056 underpin reward-seeking behaviour in humans. Nature 442:1042–1045.

1057 Qiao L, Zhang L, Chen A, Egner T (2017) Dynamic Trial-by-Trial Recoding of Task-Set Representations in
1058 the Frontoparietal Cortex Mediates Behavioral Flexibility. J Neurosci 37:11037–11050.

1059 Rouder JN, Speckman PL, Sun D, Morey RD, Iverson G (2009) Bayesian tests for accepting and rejecting
1060 the null hypothesis. Psychon Bull Rev 16:225–237.

1061 Rowe J, Hughes L, Eckstein D, Owen AM (2008) Rule-Selection and Action-Selection have a Shared
1062 Neuroanatomical Basis in the Human Prefrontal and Parietal Cortex. Cereb Cortex N Y NY
1063 18:2275–2285.

1064 Rubinstein JS, Meyer DE, Evans JE (2001) Executive control of cognitive processes in task switching. J Exp
1065 Psychol Hum Percept Perform 27:763–797.

1066 Ruge H, Braver T, Meiran N (2009) Attention, intention, and strategy in preparatory control.
1067 Neuropsychologia 47:1670–1685.

1068 Rutledge RB, Dean M, Caplin A, Glimcher PW (2010) Testing the Reward Prediction Error Hypothesis
1069 with an Axiomatic Model. J Neurosci 30:13525–13536.

1070 Schultz W (2016) Dopamine reward prediction-error signalling: a two-component response. Nat Rev
1071 Neurosci 17:183–195.

1072 Sigala N, Kusunoki M, Nimmo-Smith I, Gaffan D, Duncan J (2008) Hierarchical coding for sequential task
1073 events in the monkey prefrontal cortex. Proc Natl Acad Sci 105:11969–11974.

1074 Soon CS, Brass M, Heinze H-J, Haynes J-D (2008) Unconscious determinants of free decisions in the
1075 human brain. Nat Neurosci 11:543–545.

1076 Soon CS, He AH, Bode S, Haynes J-D (2013) Predicting free choices for abstract intentions. Proc Natl Acad
1077 Sci 110:6217–6222.

1078 Sperduti M, Delaveau P, Fossati P, Nadel J (2011) Different brain structures related to self- and external-
1079 agency attribution: a brief review and meta-analysis. Brain Struct Funct 216:151–157.

1080 Stokes MG, Kusunoki M, Sigala N, Nili H, Gaffan D, Duncan J (2013) Dynamic Coding for Cognitive Control
1081 in Prefrontal Cortex. Neuron 78:364–375.

1082 Sugrue LP (2004) Matching Behavior and the Representation of Value in the Parietal Cortex. Science
1083 304:1782–1787.

1084 Sutton RS, Barto AG (1990) Time-derivative models of Pavlovian reinforcement. In: Learning and
1085 computational neuroscience: Foundations of adaptive networks (Gabriel M, Moore J, eds), pp
1086 497–537. Cambridge, MA, US: The MIT Press.

1087 Taylor SF, Welsh RC, Wager TD, Luan Phan K, Fitzgerald KD, Gehring WJ (2004) A functional
1088 neuroimaging study of motivation and executive function. NeuroImage 21:1045–1054.

1089 Thurley K, Senn W, Lüscher H-R (2008) Dopamine Increases the Gain of the Input-Output Response of
1090 Rat Prefrontal Pyramidal Neurons. J Neurophysiol 99:2985–2997.

1091 Tobler PN, Fiorillo CD, Schultz W (2005) Adaptive Coding of Reward Value by Dopamine Neurons.
1092 Science 307:1642–1645.

1093 Todd MT, Nystrom LE, Cohen JD (2013) Confounds in multivariate pattern analysis: Theory and rule
1094 representation case study. NeuroImage 77:157–165.

1095 Torrubia R, Ávila C, Moltó J, Caseras X (2001) The Sensitivity to Punishment and Sensitivity to Reward
1096 Questionnaire (SPSRQ) as a measure of Gray's anxiety and impulsivity dimensions. Personal
1097 Individ Differ 31:837–862.

1098 Tricomi EM, Delgado MR, Fiez JA (2004) Modulation of Caudate Activity by Action Contingency. Neuron
1099 41:281–292.

1100 Vassena E, Krebs RM, Silvetti M, Fias W, Verguts T (2014) Dissociating contributions of ACC and vmPFC in
1101 reward prediction, outcome, and choice. Neuropsychologia 59:112–123.

1102 Viard A, Doeller CF, Hartley T, Bird CM, Burgess N (2011) Anterior Hippocampus and Goal-Directed
1103 Spatial Decision Making. J Neurosci 31:4613–4621.

1104 Volz KG, Schubotz RI, von Cramon DY (2003) Predicting events of varying probability: uncertainty
1105 investigated by fMRI. NeuroImage 19:271–280.

1106 Wagenmakers E-J (2007) A practical solution to the pervasive problems of p values. Psychon Bull Rev
1107 14:779–804.

1108 Walton ME, Croxson PL, Behrens TEJ, Kennerley SW, Rushworth MFS (2007) Adaptive decision making
1109 and value in the anterior cingulate cortex. NeuroImage 36:T142–T154.

1110 Waskom ML, Kumaran D, Gordon AM, Rissman J, Wagner AD (2014) Frontoparietal Representations of
1111 Task Context Support the Flexible Control of Goal-Directed Cognition. J Neurosci 34:10743–
1112 10755.

1113 Wisniewski D, Goschke T, Haynes J-D (2016) Similar coding of freely chosen and externally cued
1114 intentions in a fronto-parietal network. NeuroImage 134:450–458.

1115 Wisniewski D, Reverberi C, Momennejad I, Kahnt T, Haynes J-D (2015a) The Role of the Parietal Cortex in
1116 the Representation of Task–Reward Associations. J Neurosci 35:12355–12365.

1117 Wisniewski D, Reverberi C, Tusche A, Haynes J-D (2015b) The Neural Representation of Voluntary Task-
1118 Set Selection in Dynamic Environments. Cereb Cortex 25:4715–4726.

1119 Woolgar A, Afshar S, Williams MA, Rich AN (2015) Flexible Coding of Task Rules in Frontoparietal Cortex:
1120 An Adaptive System for Flexible Cognitive Control. J Cogn Neurosci:1–17.

1121 Woolgar A, Golland P, Bode S (2014) Coping with confounds in multivoxel pattern analysis: What should
1122 we do about reaction time differences? A comment on Todd, Nystrom & Cohen 2013.
1123 NeuroImage 98:506–512.

1124 Zhang J, Kriegeskorte N, Carlin JD, Rowe JB (2013) Choosing the Rules: Distinct and Overlapping
1125 Frontoparietal Representations of Task Rules for Perceptual Decisions. J Neurosci 33:11852–
1126 11862.

1127

Supplementary Material

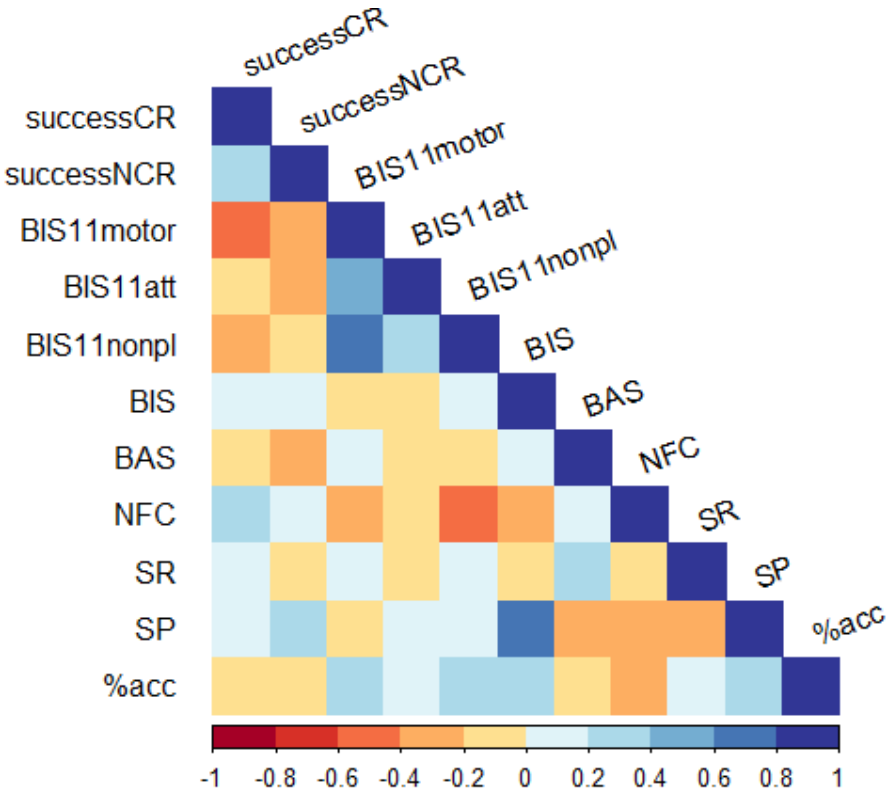

Supplementary Figure 1: Correlation analysis. An additional exploratory analysis was performed to correlate performance, questionnaire measures, and decoding accuracies (baseline task decoding, from the parietal cortex cluster). Depicted are all pairwise correlations between % high reward choices in CR trials (successCR), % high reward chocies in NCR trials (successNCR), motor impulsivity (BIS11motor), attentional impulsivity (BIS11att), non-planning impulsivity (BIS11nonpl), behavioral inhibition (BIS), behavioral approach (BAS), need for cognition (NFC), sensitivity to reward (SR), sensitivity to punishment (SP), and decoding accuracies in the baseline task decoding analysis in the parietal cortex (%acc). The plot was generated using the *corrplot* package in R.

Despite this descriptive approach, we also tested the strength of these correlations in a Bayesian framework (using *bayes.cor.test* form the BayesianFirstAid package in R). Although our conclusions are based on this correlation analysis, we also report classically estimated correlations and corresponding p-values for the interested reader. We expected successful performance to be correlated with higher need for cognition, lower impulsivity, and higher sensitivity to reward. We also expected task coding to be related to task performance, with better performance related to higher accuracies. Higher accuracies could also be related to lower impulsivity, higher sensitivity to reward, and higher need for cognition. Successful performance was correlated with impulsivity, as measured using the BIS11, r = -.34 (95%CI = [-.62 -.024]; classical estimation r = -.33, p = 0.052), with impulsive subjects being less successful in

performing the reversal learning task. The BIS11 further splits impulsivity into three components: attentional, motor, and non-planning impulsivity. The observed correlation was mostly driven by motor impulsivity (r = -.45, 95%CI = [-.70 -.15]; r = -.47, p = 0.004), but not by non-planning (r = -.19, 95%CI = [-.52 .14]; r = -.20, p = 0.24) or attentional impulsivity (r = -.11, 95%CI = [-.45 .02]; r = -.11, p = 0.51). There was no correlation of success with either sensitivity to reward (r = .04, 95%CI = [-.29 .38]; r = .06, p = 0.71), or the need for cognition (r = .26, 95%CI = [-.07 .56]; r = .26, p = 0.11), despite the fact the need for cognition seems to be associated with reward decision-making (Sandra and Otto 2018). A qualitatively similar pattern was evident for decoding accuracies, extracted during intention maintenance from the parietal cortex. Correlations with impulsivity (r = -.27, 95%CI = [-.57 .07]; r = -.32, p = 0.053), sensitivity to reward (r = -.04, 95%CI = [-.38 .31], r = .17, p = 0.30), and need for cognition (r = .09, 95%CI = [-.24 .41]; r = -.24, p – 0.16) were at least similar numerically to the correlations with task success. Given that the evidence was somewhat weaker in this analysis, results should be interpreted with care however. Overall, task performance and to a lesser degree decoding accuracies seem to be most strongly related to impulsivity, and not to sensitivity to reward or need for cognition. This unexpected link to impulsivity should be addressed directly in future research.

Sandra, D.A., & Otto A.R. (2018) Cognitive Capacity Limitations and Need for Cognition Differentially Predict Reward-Induced Cognitive Effort Expenditure. *Cognition,* 172: 101–6.

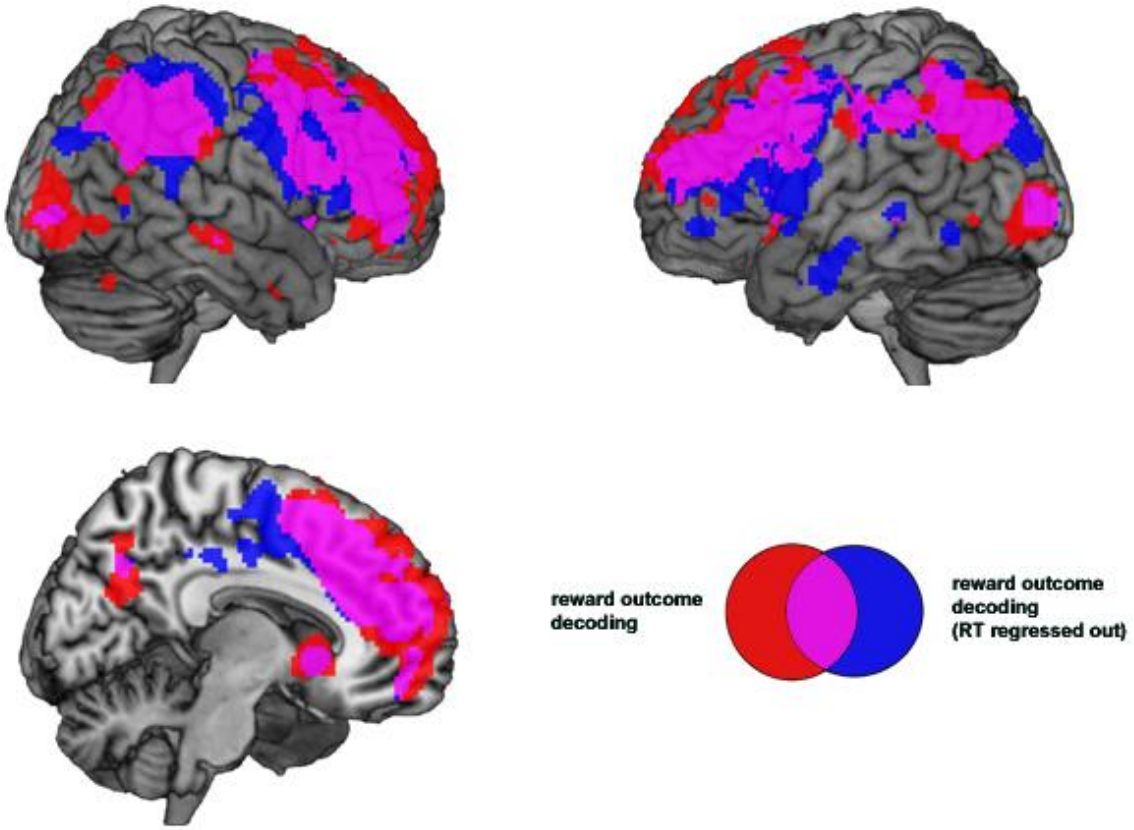

Supplementary Figure 2. Controlling RT-effects in reward outcome coding. We repeated the reward outcome decoding analysis, using a similar first-level GLM to estimate signals (4 regressors: each combination of high vs low reward, contingent vs non-contingent reward, locked to feedback onset). Additionally, we added regressors of non-interest capturing RT-related variance in the data. The rest of the analysis was identical to the reward outcome decoding analysis presented in the main body of the text. Results from the reward outcome decoding analysis (red), and the same analysis with RT-related effects regressed out of the data (blue) are depicted. As can be seen, the overlap between both analyses is substantial. Results depicted at $p < 0.05$ (FWE, corrected at the voxel level). This indicates that controlling for RT did not strongly alter our results.

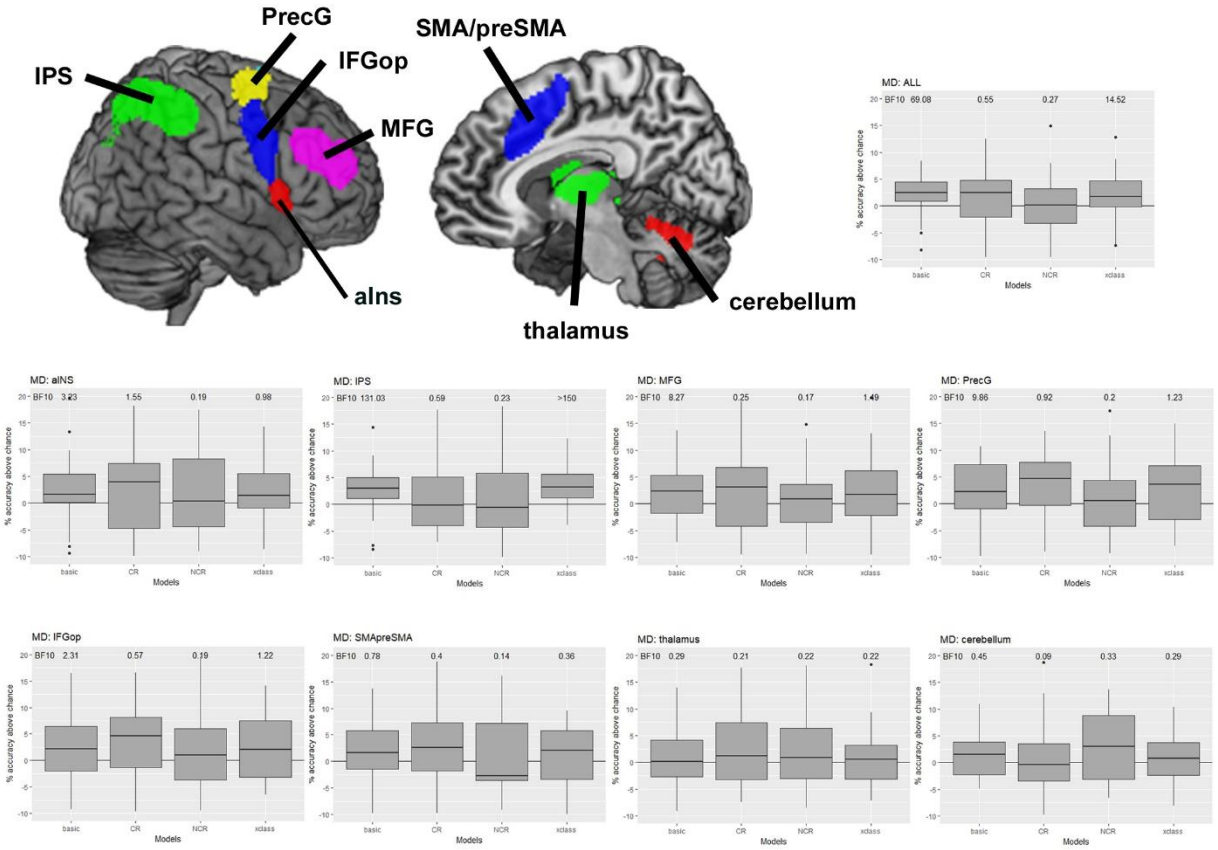

Supplementary Figure 3. Task information in the multiple demand (MD) network. Depicted are task decoding results in the bilateral functional ROIS provided by Fedorenko, Duncan, & Kanwisher (2013), specifically the anterior insula (aINS), cerebellum, inferior frontal gyrus pars opercularis (IFGop), intraparietal sulcus (IPS), middle frontal gyrus (MFG), pre-central gyrus (precG), supplementary and pre-supplementary motor area (SMA/preSMA), as well as thalamus. Averaging across all MD regions, we found strong evidence for the presence of task information (2.23%, SEM = 0.61%, BF10 = 69.08, t(34) = 3.63, p < 0.001, Figure 1). We then tested whether accuracies were higher in CR trials than in NCR trials, using the same analysis as used for the regions identified in the main task decoding analysis. We found no evidence for a higher accuracy in CR, as compared to NCR trials (BF10 = 0.37, t(34) = 0.68, p = 0.24). Furthermore, we found task coding to be contingency-invariant, using a cross-classification approach (2.02%, SEM = 0.67%, BF10 = 14.52, t(34) = 2.97, p = 0.002). Accuracies in the baseline and cross-classification analysis did not differ (BF10 = 5.11, t(34) = 0.40, p = 0.68). This suggests that the MD network encodes tasks in a contingency-invariant fashion, and shows that the current context does not affect task coding in the MD network. This is despite the clear effects contingency has on the coding of reward outcomes.

Looking at individual MD regions, we found task information in the aINS (2.25%, SEM = 1.00%, BF10 = 3.23, t(34) = 2.24, p = 0.01), IPS (2.83%, SEM = 0.72%, BF10 = 131.02, t(34) = 3.88, p < 0.001), MFG (2.44%, SEM = 0.90%, BF10 = 8.26, t(34) = 2.71, p = 0.005), precentral gyrus (2.48%, SEM = 0.87, BF10 = 9.86, t(34)

= 2.79, p = 0.004), but not in the cerebellum (0.85%, SEM = 0.90%, BF10 = 0.44, t(34) = 0.94, p = 0.17), IFGop (2.11%, SEM = 1.02%, BF10 = 2.31, t(34) = 2.06, p = 0.02) SMA/preSMA (1.48%, SEM = 1.07%, BF10 = 0.77, t(34) = 1.37, p = 0.08), and thalamus (0.58%, SEM = 1.06%, BF10 = 0.29, t(34) = 0.54, p = 0.29). None of these regions showed a higher accuracy in CR than in NCR trials (BFs10 <= 0.60, ts(34) < 1.19, ps > 0.12). However, in all of those regions the accuracy in the baseline and xclass analyses was equal (BFs10 >= 3.47, ts(34) < 1.00, ps > 0.32). In sum, we did not find our reward manipulation to affect task coding in the MD network. We did find contingency-invariant task information in this network however. Also, not all parts of the MD network seemed to be encoding tasks in our experiment.

Fedorenko E, Duncan J, Kanwisher N. 2013. Broad domain generality in focal regions of frontal and parietal cortex. P Natl Acad Sci USA. 110:16616–16621.